

Geometric Quantum Thermodynamic Engine under an Isothermal Operation: An Application of a Thouless Pumping

Ryosuke Yoshii*

*Center for Liberal Arts and Sciences, Sanyo-Onoda City University, Yamaguchi 756-0884, Japan, and
International Institute for Sustainability with Knotted Chiral Meta Matter (WPI-SKCM2),
Hiroshima University, Higashi-Hiroshima, Hiroshima 739-8526, Japan*

Hisao Hayakawa†

*Center of Gravitational Physics and Quantum Information,
Yukawa Institute for Theoretical Physics, Kyoto University,
Kitashirakawa-oiwake cho, Sakyo-ku, Kyoto 606-8502, Japan*

(Dated: June 7, 2025)

We present a geometric formalism for the non-equilibrium thermodynamics of a small system coupled to external isothermal reservoirs as an application of Thouless pumping, where the electrochemical potentials of the reservoirs and parameters in the system's Hamiltonian are adiabatically controlled. By analyzing the quantum master equation for the Anderson model of a quantum dot under the wide-band approximation, we obtain the work and effective efficiency of the thermodynamic engine as functions of the phase difference between the externally controlled electrochemical potentials after the system reaches a geometric cyclic state. Since the entropy production is negligible in adiabatic operations, the process we consider is reversible, analogous to the Carnot cycle.

I. INTRODUCTION

Since Thouless first introduced the concept of adiabatic geometric pumping [1, 2], it has been established that a current can flow without an average bias when a Berry-phase-like variable or Berry-Sinitsyn-Nemenman (BSN) curvature emerges in the space of modulation parameters [1–6]. This phenomenon, widely known as Thouless pumping or geometric pumping, has been experimentally validated in processes such as charge transport [7–14] and spin pumping [15]. Theoretical studies have explored this effect using diverse methodologies, including scattering theories [16–23], classical master equations [24–33], and quantum master equations [34–39]. Extended fluctuation theorems for geometric pumping have also been investigated [40–42], enriching the theoretical framework.

Geometric pumping has profound implications for nanoscale thermodynamics, particularly in the context of finite-time processes [43], where thermodynamic length is a pivotal concept. Originally developed for macroscopic systems [44–48], thermodynamic length has since been adapted to classical nanoscale systems [49], closed quantum systems [50], and open quantum systems [51]. These concepts are especially pertinent to quantum thermodynamics and the design of nanoscale machines [52–54]. A recent review [55] highlights the essential role of geometric formulations in understanding and manipulating such systems.

Several studies have sought to develop a geometric thermodynamics framework for microscopic heat engines operating in the adiabatic regime [56–63]. Notably, Hino and Hayakawa [58] proposed a geometric theory for a heat engine driven by BSN curvature, operating without an average temperature difference between two reservoirs. However, this approach has limitations: it is confined to systems described by classical master equations, thus neglecting quantum effects, and the periodic control of reservoir temperatures presents experimental difficulties. Substituting temperature modulation with control of electrochemical potentials offers a more experimentally feasible approach compared to temperature control.

In this work, we propose an isothermal engine that modulates the electrochemical potentials of reservoirs and parameters in the system's Hamiltonian. This study builds upon Ref. [64], which explored initial relaxation from a nonequilibrium steady state, whereas we examine the system's behavior after reaching a geometric state. The dissipative availability is zero since temperature remains constant and the system's dynamics are fully reversible in this scenario. Although Ref. [63] developed a geometric thermodynamics around the geometric state (they call the cyclic state), the authors of Ref. [63] focus on states slightly deviated from the cyclic state, mainly from non-adiabatic effects. Thus, the system they considered contains irreversibility caused by the entropy production, while we operate the system adiabatically without the entropy production to keep the local reversibility. This is the main difference between our approach and that of Ref. [63].

* e-mail address: ryoshii@rs.socu.ac.jp

† e-mail address: hisao@yukawa.kyoto-u.ac.jp

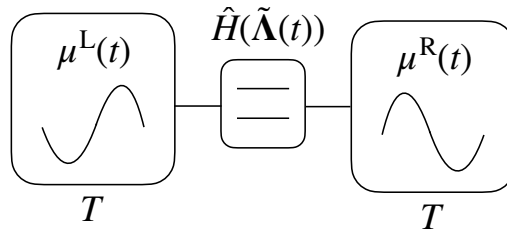


Figure 1. A schematic of the model we consider in this paper, in which $\mu^L(t)$, $\mu^R(t)$, and $\hat{H}(\tilde{\Lambda}(t))$ are modulated by an external agent.

We apply the geometric thermodynamics to the Anderson model—a single quantum dot system governed by a quantum master equation under the wide-band approximation [64, 65]. This approach enables us to incorporate quantum effects and provides a practical framework for analyzing nanoscale thermodynamic engines. In particular, we focus on the adiabatic process in which the density matrix always satisfies the geometric state [64] and the Kullback–Leibler (KL) divergence [66, 67] is always zero. Namely, we are interested in a reversible thermodynamic engine corresponding to the Carnot cycle.

The organization of this paper is as follows. In Sec. II, we explain the setup and a geometric formulation for describing the heat engine under an adiabatic pumping process, including the descriptions of the first law of thermodynamics in our system. In Sec. III, we apply our formulation to the Anderson model for a quantum dot coupled to two reservoirs within the wide-band approximation. In Sec. IV, we present our results based on the calculation for the Anderson model. Finally, in Sec. V we summarize our results and perspectives with some discussions. In Appendix A, we explicitly write the eigenvalues and eigenvectors of the Anderson model. In Appendix B, we derive the transition matrix of a quantum master equation for the Anderson model. In Appendix C, we try to evaluate the cost of manipulating engines cyclically. In Appendix D, we obtain the electric current under a cyclic modulation with the aid of the counting field.

II. GENERAL FRAMEWORK

In this section, we develop a general framework for describing the thermodynamics of a quantum system under adiabatic pumping. We first outline the system setup (Section II A) and then derive the first law of thermodynamics in the context of geometric cyclic states (Section II B).

A. Setup

In this paper, we consider a small quantum system S such as a quantum dot coupled to two reservoirs L and R under periodic modulation of some system parameters, with the period τ_p . We focus on the isothermal condition throughout this study. Each reservoir $\alpha = \text{L or R}$ is characterized by the electrochemical potential μ^α and temperature T (or the inverse temperature $\beta := 1/T$). In this paper, we adopt natural units where the Boltzmann constant $k_B = 1$, such that temperature T has the dimension of energy, and we also set the Planck constant $\hbar = 1$.

Although our general formalism can be applied to many systems, we specify the model employed in this paper for the reader. We illustrate the setup by a schematic picture in Fig. 1 where we modulate $\mu^L(t)$ and $\mu^R(t)$ in the reservoirs in time t with different phases. In this paper, we control the set of parameters

$$\Lambda(t) := \left(\tilde{\Lambda}(t), \frac{\mu^L(t)}{\mu^L}, \frac{\mu^R(t)}{\mu^R} \right), \quad (1)$$

where we have introduced

$$\overline{\mu^\alpha} := \frac{1}{\tau_p} \int_0^{\tau_p} dt \mu^\alpha(t) \quad (2)$$

for $\alpha = \text{L and R}$. Here $\tilde{\Lambda}(t)$ denotes a set of parameters $\tilde{\Lambda}(t) = (\lambda_\nu(t))$ with ν -th component $\lambda_\nu(t)$ inside the quantum dot. When we consider the case without any difference in time-averaged electrochemical potentials, i.e. $\overline{\mu^R} = \overline{\mu^L}$, we can replace $\overline{\mu^\alpha}$ in Eq. (1) by $\overline{\mu}$ which is independent of α .

We assume that the quantum master equation describes the dynamics of S

$$\frac{d}{d\theta}|\hat{\rho}(\theta)\rangle = \epsilon^{-1}\hat{K}(\mathbf{\Lambda}(\theta))|\hat{\rho}(\theta)\rangle, \quad (3)$$

where $\hat{\rho}(\theta)$ is the density matrix of the system S.¹ In this study, we introduce the dimensionless time, defined as the phase of the modulation, $\theta := 2\pi t/\tau_p$, and the dimensionless operation speed, $\epsilon := 1/(\tau_p\Gamma)$, where the parameter modulation commences at $t = 0$, and Γ represents the coupling strength or the characteristic transition rate between the system and its reservoirs. A previous work [64] investigated relaxation from a nonequilibrium steady state to a geometric state, demonstrating that such relaxation generates entropy production and enables work extraction. Additionally, we note that the dynamics governed by physically relevant quantum master equations are completely positive and trace-preserving (CPTP), as established in prior studies [67–69]. Furthermore, we assume that the master equation, Eq. (3), is of the Markovian type, although the modulation incorporated in $\hat{K}(\mathbf{\Lambda}(\theta))$ through $\mathbf{\Lambda}(\theta)$ may introduce non-Markovian effects, as discussed in Ref. [70].² Given our focus on dynamics under slow modulations, we posit that the dynamic evolution of the density matrix $\hat{\rho}(\theta)$ is primarily driven by variations in $\mathbf{\Lambda}(\theta)$. When the diagonal elements of the density matrix $\hat{\rho}(\theta)$ are decoupled from the off-diagonal elements, the system exhibits classical behavior; however, if the diagonal and off-diagonal elements are coupled, the system is inherently quantum.

In Eq. (3) we have introduced the vector consisting of the elements of the density matrix

$$|\hat{\rho}(\theta)\rangle := \begin{pmatrix} \rho_{11}(\theta) \\ \rho_{12}(\theta) \\ \dots \\ \rho_{NN}(\theta) \end{pmatrix}, \quad (4)$$

where $\rho_{ij}(\theta)$ is the (ij) -element of $\hat{\rho}$ at θ , which is assumed to be a $N \times N$ matrix. We note that the diagonal element appears at the $M + N(M - 1)$ -th component ($1 \leq M \leq N$). The density matrix $\hat{\rho}(\theta)$ satisfies the condition of probability conservation $\text{Tr}\hat{\rho}(\theta) = 1$. Thus, the transition matrix $\hat{K}(\mathbf{\Lambda}(\theta))$ is a superoperator acting on $|\hat{\rho}(\theta)\rangle$, which is expressed as a $N^2 \times N^2$ matrix.

We assume that the master equation (3) has a unique steady state $|\hat{\rho}^{\text{ss}}(\mathbf{\Lambda}(\theta))\rangle$ which satisfies

$$\hat{K}(\mathbf{\Lambda}(\theta))|\hat{\rho}^{\text{ss}}(\mathbf{\Lambda}(\theta))\rangle = 0. \quad (5)$$

Equation (5) means that the steady density matrix is equivalent to the right zero eigenstate of $\hat{K}(\mathbf{\Lambda}(\theta))$. Since the system is coupled to two reservoirs having different electrochemical potentials, $|\hat{\rho}^{\text{ss}}(\mathbf{\Lambda}(\theta))\rangle$ is a nonequilibrium steady state in the presence of the bias voltages. In the following, we denote the left zero eigenvector of $\hat{K}(\mathbf{\Lambda}(\theta))$ as $\langle\ell_0|$, which satisfies $\langle\ell_0|\hat{\rho}^{\text{ss}}(\mathbf{\Lambda}(\theta))\rangle = \text{Tr}\hat{\rho}^{\text{ss}}(\mathbf{\Lambda}(\theta)) = 1$. This transition matrix has n^2 eigenvalues ε_i and corresponding eigenvectors. Since the transition matrix is non-Hermitian, the left eigenstates $\langle\ell_i|$ and right eigenstates $|r_i\rangle$ with the eigenvalue ε_i are not the Hermitian conjugate. For later convenience, we label the eigenvalues ε_i such that $\varepsilon_0 = 0 > \text{Re}[\varepsilon_1] \geq \text{Re}[\varepsilon_2] \geq \dots \geq \text{Re}[\varepsilon_{n^2-1}]$, where $\text{Re}[\varepsilon_i]$ represents the real part of ε_i . In this convention, the 0-th eigenvector coincides with the steady state vector $|r_0\rangle = |\hat{\rho}^{\text{ss}}(\mathbf{\Lambda}(\theta))\rangle$.

As shown in Ref. [64], the state rapidly relaxes to the geometric cyclic state. In the presence of a slow modulation ($\epsilon \rightarrow 0$), the correction of the state vector $|\hat{\rho}\rangle$ from the steady state $|\hat{\rho}^{\text{ss}}\rangle$ can be expressed as an adiabatically modulated geometric phase. When the eigenvalues of $\hat{K}(\mathbf{\Lambda}(\theta))$ do not have any degeneracy, the state vector $|\hat{\rho}(\theta)\rangle$ is given by

$$|\hat{\rho}(\theta)\rangle \simeq |\hat{\rho}^{\text{ss}}(\theta)\rangle := |\hat{\rho}^{\text{ss}}(\theta)\rangle + \epsilon \sum_{i \neq 0}^{N^2-1} C_i(\theta)|r_i(\theta)\rangle, \quad (6)$$

where

$$C_i(\theta) := -\frac{1}{\epsilon} \int_0^\theta d\phi e^{\epsilon^{-1} \int_\phi^\theta dz \varepsilon_i(z)} \langle\ell_i(\phi)| \frac{d}{d\phi} |\hat{\rho}^{\text{ss}}(\phi)\rangle. \quad (7)$$

The second term on the RHS of Eq. (6) is the Berry-Sinitsyn-Nemenman (BSN) connection [5, 6]. The error of the expression in Eq. (6) is $O(\epsilon^2)$, but similar expressions can be found even in non-adiabatic cases as in Refs. [72, 73].

¹ We adopt a simplified notation $\mathbf{\Lambda}(\theta) = \mathbf{\Lambda}(t)$.

² Gorini–Kossakowski–Sudarshan–Lindblad equation with non-negative jump rates is CP-divisible even if some jump rates are negative. However, some convolution-less master equations are non-Markovian, and time-dependent jump rates might be negative [71].

Note that geometric cyclic state $|\hat{\rho}^{\text{gs}}\rangle$ in Eqs. (6) and (7) can be used after the initial relaxation process ($\theta \gg \epsilon$) without entropy (KL-divergence) production as shown in Ref. [64]. Although the expression in Eqs. (6) and (7) cannot be used if the eigenvalues are of $\hat{K}(\Lambda(\theta))$ degenerated, we may use the approximate expression:

$$|\hat{\rho}^{\text{gs}}(\theta)\rangle \simeq |\hat{\rho}^{\text{ss}}(\theta)\rangle + \epsilon \sum_{i=1}^{\mathcal{M}} C_i(\theta) |r_i(\theta)\rangle, \quad (8)$$

when the degeneracy exists only in the \mathcal{M} -th. excited state with well-separated eigenvalues as $\epsilon_{\mathcal{M}} - \epsilon_{\mathcal{M}-1} \gg \epsilon$ with $\mathcal{M} \leq N^2 - 1$.

The expression (7) has an intuitive interpretation. If we consider the slow modulating limit $\epsilon \ll \epsilon_i(z) (\forall z, 1 \leq i \leq \mathcal{M})$, the integrand of Eq. (7) is zero except for $|\epsilon_i(\theta - \phi)| < \epsilon$. In other words, the exponential factor works as the cut-off factor. Thus Eq. (7) can be approximated as

$$C_i(\theta) \simeq -\frac{1}{\epsilon} \int_{\theta - |\epsilon/\epsilon_i|}^{\theta} d\phi e^{\epsilon^{-1} \int_{\phi}^{\theta} dz \epsilon_i(z)} \langle \ell_i(\phi) | \frac{d}{d\phi} | \hat{\rho}^{\text{ss}}(\phi) \rangle \simeq -\frac{1}{\bar{\epsilon}_i} \langle \ell_i(\theta) | \frac{d}{d\theta} | \hat{\rho}^{\text{ss}}(\theta) \rangle + O(\epsilon), \quad (9)$$

where we use the following approximation.

$$e^{\epsilon^{-1} \int_{\phi}^{\theta} dz \epsilon_i(z)} \simeq e^{\epsilon^{-1} \bar{\epsilon}_i (\theta - \phi)}, \quad (10)$$

where we define the averaged eigenvalue as follows.

$$\bar{\epsilon}_i := \frac{1}{\theta - \phi} \int_{\phi}^{\theta} dz \epsilon_i(z). \quad (11)$$

It is remarkable that the coefficient $C_i(\theta)$ is independent of ϵ for slow modulations. Note that $C_i(\theta)$ with a large eigenvalue is irrelevant for the slow dynamics. Substituting Eq. (9) into Eq. (8) with neglecting the contribution of $C_i(\theta)$ for $i \geq 2$, we obtain

$$|\hat{\rho}^{\text{gs}}(\theta)\rangle \simeq |\hat{\rho}^{\text{ss}}(\theta)\rangle - \frac{\epsilon}{\bar{\epsilon}_1} |r_1(\theta)\rangle \langle \ell_1(\theta) | \frac{d}{d\theta} | \hat{\rho}^{\text{ss}}(\theta) \rangle + O(\epsilon^2). \quad (12)$$

Equation (12) is similar to the Born approximation in scattering theory.

B. First law of thermodynamics

Now, we discuss the thermodynamic relations for our system. First, we consider the first law of thermodynamics [64, 74–76]. The energy of the subsystem is given by

$$E(\theta) := \text{Tr}[\hat{H}(\tilde{\Lambda}(\theta)) \hat{\rho}(\theta)]. \quad (13)$$

The rate of change of internal energy is given by

$$\frac{dE}{d\theta}(\theta) = \mathcal{P}(\theta) + \mathcal{J}(\theta), \quad (14)$$

where $\mathcal{P}(\theta)$ and $\mathcal{J}(\theta)$ appearing in the right hand side are The power and the heat current are explained below. The power $\mathcal{P}(\theta)$ is defined as

$$\mathcal{P}(\theta) := \text{Tr} \left[\hat{\rho}(\theta) \frac{d\hat{H}(\tilde{\Lambda}(\theta))}{d\theta} \right]. \quad (15)$$

The second term on the RHS of Eq. (14) is the heat flow defined as

$$\mathcal{J}(\theta) := \text{Tr} \left[\hat{H}(\tilde{\Lambda}(\theta)) \frac{d\hat{\rho}(\theta)}{d\theta} \right]. \quad (16)$$

Let us rewrite Eq. (16). Using $\langle \ell_0 | = \sum_{\mu=1}^N (\mu | \otimes | \mu \rangle$, we have the relation:

$$\begin{aligned} \left\langle \ell_0 \left| \hat{H} \left| \frac{d\hat{\rho}}{d\theta} \right. \right\rangle &= \sum_{\mu, \nu, \sigma, \chi, \xi=1}^N (\mu | h_{\chi, \xi} | \chi \rangle \langle \xi | \left(\frac{d\rho_{\nu, \sigma}}{d\theta} | \nu \rangle \langle \sigma | \right) | \mu \rangle = \sum_{\mu, \nu, \sigma, \chi, \xi=1}^N h_{\chi, \xi} \frac{d\rho_{\nu, \sigma}}{d\theta} \delta_{\mu\chi} \delta_{\xi, \nu} \delta_{\sigma, \mu} \\ &= \sum_{\mu, \nu=1}^N h_{\mu, \nu} \frac{d\rho_{\nu, \mu}}{d\theta} = \text{Tr} \left[\hat{H} \frac{d\hat{\rho}}{d\theta} \right], \end{aligned} \quad (17)$$

where $\{|\mu\rangle\}$ and $\{|\nu\rangle\}$ are complete orthonormal sets in the Hilbert space of \hat{H} satisfying the completeness relation $\sum_{\mu} |\mu\rangle \langle \mu| = 1$ and the orthonormal condition $(\mu | \nu) = \delta_{\mu, \nu}$. Here, we also introduced $h_{\chi, \xi} := (\chi | \hat{H} | \xi)$, and $\rho_{\nu, \sigma} := (\nu | \hat{\rho} | \sigma)$. With the aid of Eq. (17), Eq. (16) can be rewritten as

$$\mathcal{J}(\theta) = \langle \ell_0 | \hat{H}(\tilde{\Lambda}(\theta)) \frac{d}{d\theta} | \rho(\theta) \rangle. \quad (18)$$

To explain the explicit relationship between \hat{H} represented by the basis in the Hilbert space of \hat{H} and that in the Hilbert space of \hat{K} , let us refer to the basis of states in the Hilbert space of \hat{H} as $|m\rangle$.

The explicit form of \hat{H} for the Anderson model is given in Appendix A. Plugging Eqs. (3) and (6) into Eq. (18) and using Eq. (5), we can rewrite $\mathcal{J}(\theta)$ as

$$\mathcal{J}(\theta) = \epsilon^{-1} \langle \ell_0 | \hat{H}(\tilde{\Lambda}(\theta)) \hat{K}(\Lambda(\theta)) | \rho(\theta) \rangle = \sum_{i \neq 0}^m \varepsilon_i C_i(\theta) \langle \ell_0 | \hat{H}(\tilde{\Lambda}(\theta)) | r_i(\theta) \rangle. \quad (19)$$

Let us introduce the heat $\mathcal{Q}(\theta)$:

$$\mathcal{Q}(\theta) := \int_{\theta_{\text{in}}}^{\theta + \theta_{\text{in}}} d\theta \mathcal{J}(\theta) = \int_{\theta_{\text{in}}}^{\theta_{\text{in}} + \theta} d\phi \sum_{i \neq 0}^m \varepsilon_i C_i(\phi) \langle \ell_0 | \hat{H}(\tilde{\Lambda}(\phi)) | r_i(\phi) \rangle. \quad (20)$$

Similarly, the power can also be rewritten in the supervector representation as

$$\mathcal{P}(\theta) = \langle \ell_0 | \frac{d\hat{H}(\tilde{\Lambda}(\theta))}{d\theta} | \rho(\theta) \rangle. \quad (21)$$

Even if we start from the steady state, KL divergence is generated, as shown in Ref. [64]. The work generated in θ starting from θ_{in} becomes

$$\mathcal{W}(\theta) := \int_{\theta_{\text{in}}}^{\theta_{\text{in}} + \theta} d\phi \mathcal{P}(\phi). \quad (22)$$

By definition, the relation $\mathcal{P}(\theta) = d\mathcal{W}(\theta)/d\theta$ holds.

Since $E(\theta)$ is the single-valued function of θ , the contour integral of the left-hand side of Eq. (14) along the closed path is zero $\oint d\theta \frac{dE}{d\theta} = E(2\pi + \theta_{\text{in}}) - E(\theta_{\text{in}}) = 0$, where $\theta_{\text{in}} \gg \epsilon$ is the initial observation phase after the system reaches a geometric cyclic state. Thus we obtain the following constraint on \mathcal{P} and \mathcal{J} as

$$\oint \mathcal{P}(\theta) d\theta + \oint \mathcal{J}(\theta) d\theta = 0. \quad (23)$$

Substituting Eq. (21) into Eq. (22) with setting $\theta = 2\pi$ the work W during one cycle can be written as

$$W := \mathcal{W}(2\pi) = \int_{\theta_{\text{in}}}^{2\pi + \theta_{\text{in}}} d\phi \mathcal{P}(\phi) = \int_{\theta_{\text{in}}}^{2\pi + \theta_{\text{in}}} \langle \ell_0 | \frac{\partial \hat{H}(\tilde{\Lambda}(\phi))}{\partial \lambda_\nu} | \rho(\phi) \rangle \dot{\lambda}_\nu d\phi \quad (24)$$

where $\dot{\lambda}_\mu := d\lambda_\mu(\theta)/d\theta$, and we obey Einstein's summation convention. Introducing the vector potential A^ν defined as

$$A^\nu := \beta \langle \ell_0 | \frac{\partial \hat{H}(\tilde{\Lambda}(\phi))}{\partial \lambda_\nu} | \rho(\phi) \rangle, \quad (25)$$

we can rewrite Eq. (24) as

$$\beta W = \oint A^\nu d\lambda_\nu, \quad (26)$$

where $d\lambda_\nu := \dot{\lambda}_\nu d\theta$. Using the vector potential A^ν , the power \mathcal{P} can be expressed as

$$\beta \mathcal{P}(\theta) = A^\mu \dot{\lambda}_\mu. \quad (27)$$

The work $W(\delta)$ and power $\mathcal{P}(\theta)$ can be positive or negative depending on the situation. A positive $\mathcal{P}(\theta)$ is interpreted as a power input from the external agent, while a negative $\mathcal{P}(\theta)$ can be interpreted as a power loss. By using the Stokes' theorem, Eq. (26) can be rewritten as

$$\beta W = \int_\gamma F^{\nu\sigma} dS_{\nu\sigma}, \quad (28)$$

where γ and $\partial\gamma$ are the area enclosed by the trajectory in the parameter space and whose boundary, respectively. Here we define $S_{\nu\sigma} = \frac{1}{2}d\lambda_\nu \wedge d\lambda_\sigma$ and the curvature $F^{\nu\sigma}$ defined as follows.

$$F^{\nu\sigma} := \frac{\partial A^\nu}{\partial \lambda_\sigma} - \frac{\partial A^\sigma}{\partial \lambda_\nu}. \quad (29)$$

Similarly, using Eq. (20), the heat generated in the time duration θ becomes

$$\mathcal{Q}(\theta) = \int_{\theta_{\text{in}}}^{\theta_{\text{in}}+\theta} d\phi \frac{dE}{d\phi} - \int_{\theta_{\text{in}}}^{\theta_{\text{in}}+\theta} d\phi \mathcal{P}(\phi), \quad (30)$$

where we have used Eq. (14). The heat generated during one cycle is defined as

$$Q := \mathcal{Q}(2\pi) = -W, \quad (31)$$

where we have used Eq. (23). The power $\mathcal{P}(\theta)$, the work $W(\delta)$, the heat flow $\mathcal{Q}(\theta)$, and the heat Q can be calculated once we know the density matrix $\hat{\rho}(\theta)$ as in Eqs. (8) and (9).

During parameter modulation, the system both absorbs and releases heat. We note that the total heat exchanged over one cycle balances with the work done, as per the first law of thermodynamics. Thus, there is no heat accumulation in each cycle. To define the efficiency of the present system, we divide the whole process into the heat-absorbing process ($\mathcal{J} \geq 0$) and the heat-releasing process ($\mathcal{J} < 0$) and define the absorbed heat Q_A and the released heat Q_R during the one-cycle as

$$Q_A := \int_{\theta_{\text{in}}}^{2\pi+\theta_{\text{in}}} \mathcal{J} \Theta(\mathcal{J}) d\theta, \quad (32)$$

$$Q_R := - \int_{\theta_{\text{in}}}^{2\pi+\theta_{\text{in}}} \mathcal{J} \Theta(-\mathcal{J}) d\theta, \quad (33)$$

where $\Theta(x)$ is Heaviside's step function; $\Theta(x) = 0$ for $x \leq 0$ and $\Theta(x) = 1$ otherwise. The efficiency η of the present model can be defined as

$$\eta := -\frac{W}{Q_A}. \quad (34)$$

Here, we note that the system becomes a heat engine only if the work generated during one cycle becomes negative. From the relations $Q + W = 0$ and $Q = Q_A - Q_R$ the efficiency satisfies

$$\eta = 1 - \frac{Q_R}{Q_A} \leq 1. \quad (35)$$

This relation is analogous to the Carnot efficiency in which Q_R and Q_A are replaced with the temperatures of a cold reservoir and a hot reservoir, respectively.³ Since our engine is reversible, Eq. (35) for η corresponds to the Carnot efficiency in engines under cyclic modulations.

³ It is well known that the standard thermodynamics under a quasi-static operation satisfies $Q_H/T_H = Q_C/T_C$, where Q_H , T_H , Q_C , and T_C are the absorbing heat Q_A from a hot reservoir, the temperature of the hot reservoir, the release heat Q_C to a cold reservoir, and the temperature of the cold reservoir. Thus, the Carnot efficiency can be expressed as $\eta_C = 1 - Q_C/Q_H$, which is equivalent to Eq. (35).

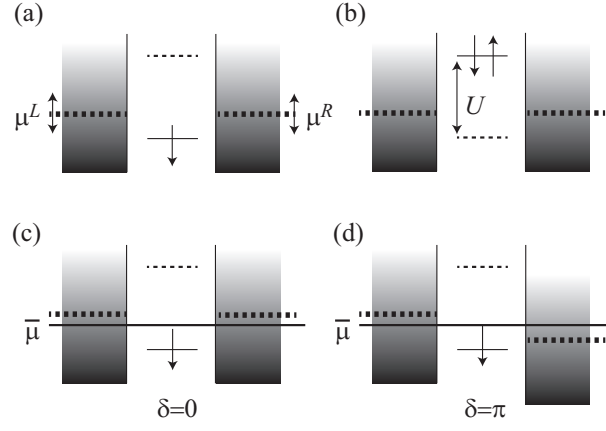


Figure 2. (a) Schematics of a modulation of the Anderson model in which two reservoirs are connected to a quantum dot. We modulate the electrochemical potentials in the left ($\mu^L(\theta)$) and right ($\mu^R(\theta)$) reservoirs. (b) We also modulate the Coulomb repulsion U inside the quantum dot as a tunable parameter. Another control parameter, δ , represents the phase difference between the modulations of the two electrochemical potentials. Figures (c) and (d) are schematics for $\delta = 0$ and $\delta = \pi$, respectively.

Although negative or positive βQ seems to be strange under an adiabatic operation, the heat defined by Eq. (20) is consistent with the second law of thermodynamics because it expresses only the heat transfer between the reservoirs and the system. As indicated in Ref. [64], KL-divergence is the most important to ensure the monotonicity of the entire system, which corresponds to the second law. In the present paper, we analyze the reversible case without any production of the KL-divergence. Even in this case, we can introduce the system entropy production to satisfy the relationship $\Delta S_{\text{sys}} = \beta Q$ to characterize the thermodynamics of the target system. However, this ΔS_{sys} does not have any monotonicity.

In summary of the formulation, we need a vector potential A^ν to describe a thermodynamic process in a cyclic modulation. So far, we have not restricted the speed of the operation. Thus, we can apply this formulation to an adiabatic process without entropy production, which may correspond to the Carnot cycle in standard thermodynamics.

III. APPLICATION TO A QUANTUM DOT SYSTEM

In this section, we apply the general framework developed in the previous section to the Anderson model for a quantum dot (QD) in which a single dot is coupled to two electron reservoirs. Figure 2 illustrates the time evolution of our system.

The total system consists of the single-dot system and baths (reservoirs). Thus, the total Hamiltonian \hat{H}^{tot} is written as

$$\hat{H}^{\text{tot}} := \hat{H} + \hat{H}^{\text{r}} + \hat{H}^{\text{int}}, \quad (36)$$

where the system Hamiltonian \hat{H} , reservoir Hamiltonian \hat{H}^{r} and interaction Hamiltonian \hat{H}^{int} are, respectively, given by

$$\hat{H} = \sum_{\sigma} \epsilon_0 \hat{d}_{\sigma}^{\dagger} \hat{d}_{\sigma} + U(\theta) \hat{n}_{\uparrow} \hat{n}_{\downarrow}. \quad (37)$$

$$\hat{H}^{\text{r}} = \sum_{\alpha, k, \sigma} \epsilon_k \hat{a}_{\alpha, k, \sigma}^{\dagger} \hat{a}_{\alpha, k, \sigma} \quad (38)$$

$$\hat{H}^{\text{int}} = \sum_{\alpha, k, \sigma} V_{\alpha} \hat{d}_{\sigma}^{\dagger} \hat{a}_{\alpha, k, \sigma} + \text{h.c.}, \quad (39)$$

where $\hat{a}_{\alpha, k, \sigma}^{\dagger}$ and $\hat{a}_{\alpha, k, \sigma}$ are, respectively, the creation and annihilation operators for the electron in the reservoirs $\alpha=(\text{L or R})$ with wave number k , energy ϵ_k , and spin $\sigma = (\uparrow \text{ or } \downarrow)$. Moreover, $\hat{d}_{\sigma}^{\dagger}$ and \hat{d}_{σ} are those in the QD, and $\hat{n}_{\sigma} = \hat{d}_{\sigma}^{\dagger} \hat{d}_{\sigma}$. Here, we assume that $\tilde{\Lambda}(\theta)$ contains only one component $\lambda_{\nu}(\theta) = \lambda(\theta) \delta_{\nu, 1}$ controlling the repulsive

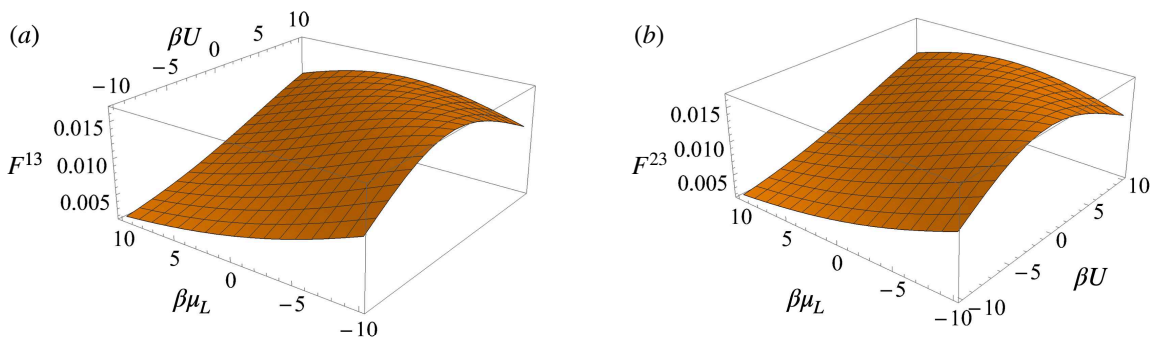


Figure 3. Plots of F^{13} (a) and F^{23} (b) as functions of μ_L and U with $\delta = 0$, respectively.

interaction $U(\theta)$ as

$$U(\theta) = U_0 \lambda(\theta). \quad (40)$$

We have introduced the transfer energy V_α between the QD and the reservoir α in Eq. (39). We adopt a model in the wide-band limit for the reservoirs. In this paper, the line width is given by $\Gamma = \pi n V^2$, where $V := \sqrt{V_L^2 + V_R^2}$ and n is the density of states in the reservoirs. For simplicity, we focus on the case of $V_L = V_R$ throughout this study.

As shown in Appendix A with explicit expressions for eigenvalues and eigenvectors, this system is non-degenerate, and off-diagonal elements of the density matrix do not play any role. See also Appendix B for the derivation of the quantum master equation and the explicit form of the transition matrix $\hat{K}(\mathbf{\Lambda}(\theta))$. Since the system is essentially classical, the transition matrix $\hat{K}(\mathbf{\Lambda}(\theta))$ satisfies the properties of transition matrices for classical stochastic processes.

IV. RESULTS

In this subsection, we calculate the thermodynamic quantities discussed in Sec. II numerically with the aid of the detailed properties of the Anderson model. In this paper, we consider geometric work generation caused by an adiabatic modulation of the parameters. As stated, we adiabatically control μ^L and μ^R with the condition $\bar{\mu} := \bar{\mu}^\alpha$ and $U(\theta)$, and fix the other parameters.

Although Ref. [60] discussed the optimal path for high efficiency and work, we adopt the following control of the set of parameters $\mathbf{\Lambda}(\theta)$ as

$$\lambda(\theta) = 1 + r_\lambda \cos \theta, \quad (41)$$

$$\frac{\mu^L(\theta)}{\bar{\mu}} = 1 + r_\mu \sin \theta, \quad (42)$$

$$\frac{\mu^R(\theta)}{\bar{\mu}} = 1 + r_\mu \sin(\theta + \delta), \quad (43)$$

where δ is the phase difference between the electrochemical potentials in the left and right reservoirs.

If we take $\delta \neq 0$, the electrochemical potential difference between the two reservoirs remains nonzero. In this case, the dynamic current proportional to chemical potential differences (bias voltage) is much larger than the geometric current. Although the average of the dynamic current over one cycle is zero, the average of the geometric current remains nonzero. If we consider $\delta = 0$, there exists only the geometric current. Thus, the geometric effect, such as the geometric current, plays an important role in our system.

First, we show the curvature in the present model. Since we have more than two parameters, we reduce the number of parameters to draw the three-dimensional picture for $F^{\nu\sigma}$. By choosing $\theta_{\text{in}} = 2\pi$, and set $r_\mu = r_\lambda$, we have two control parameters: μ_L ($= \mu_R$), and U with fixing $\delta = 0$. Figure 3 shows F^{13} and F^{23} as functions of μ_L and U . As shown in Fig. 3, a nonzero curvature results in nonzero work over one cyclic modulation, where $\bar{\varepsilon}_1 = \frac{1}{2\pi} \int_{2\pi}^{4\pi} d\theta \varepsilon_1(\theta) \simeq -1.95102$.

We also show the curvature in the r versus θ plane in Fig. 4, where we set $r_\mu = r_\lambda = r$ and δ is set to be $\pi/4$. As can be seen in this figure, $F^{\nu\sigma}$ becomes large as r increases. Thus, we can extract larger work when we modulate the system with a larger amplitude r .

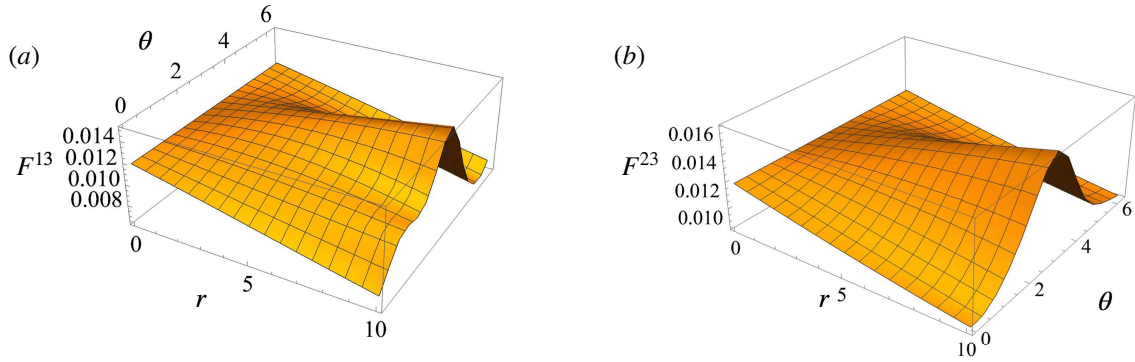


Figure 4. Plots of F^{13} (a) and F^{23} (b) as functions of $r = r_\lambda = r_\mu$ and θ , respectively, where $\delta = \pi/4$.

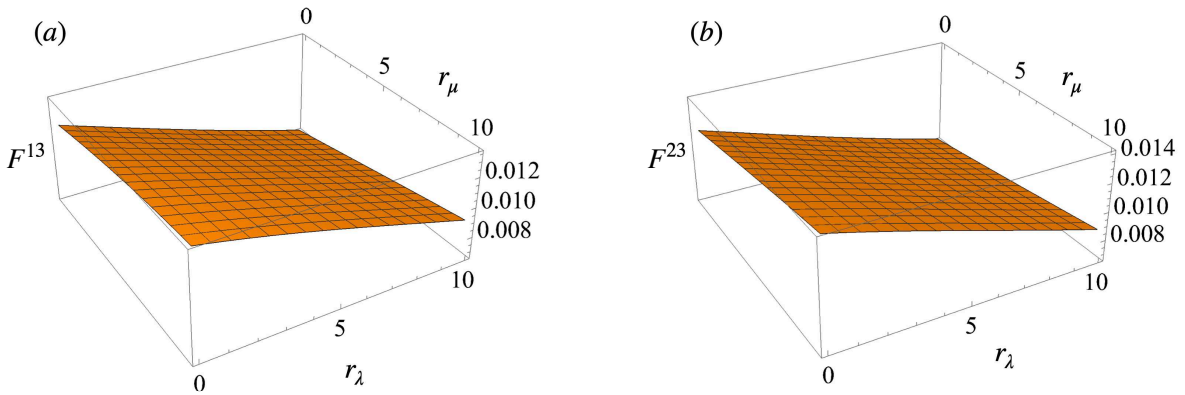


Figure 5. Plots of F^{13} (a) and F^{23} (b) as functions of r_λ and r_μ for $\theta = \pi/6$ and $\delta = \pi/4$, respectively.

To show the dependence on the magnitudes of the parameter modulations for the curvatures, we set $\theta = \pi/6$ and $\delta = 3\pi/4$ and plot the curvatures F^{13} and F^{23} as functions of r_μ and r_λ in Fig. 5. These figures suggest that $F^{\nu\sigma}$ is insensitive to r_μ but is sensitive to r_λ . Thus, the control of the Hamiltonian is important in extracting the work.

For the explicit calculation, we set $r := r_\lambda = r_\mu$ and fix the parameters $\beta\epsilon_0 = \beta\bar{\mu} = \beta U_0 = 0.1$, where ϵ_0 and U_0 are introduced in Eqs. (37) and (40), respectively. In Fig. 6, we plot θ dependence of \mathcal{P} and \mathcal{J} for $\delta = \pi/2$. As can be seen in Fig. 6(b), the heat current $\beta\mathcal{J}$ is deviated from a sinusoidal curve, which generates non-trivial work.

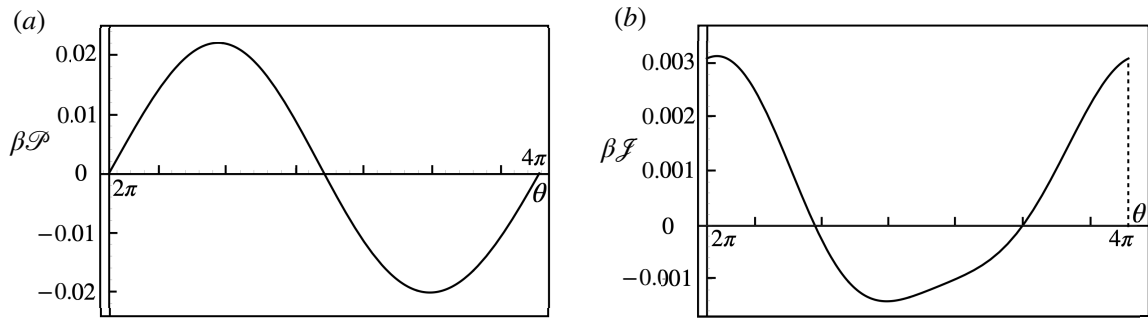


Figure 6. Plots of \mathcal{P} (a) and \mathcal{J} (b) as functions of the time θ for $r = 0.9$ with $\epsilon/|\bar{\epsilon}_1| = 0.1$, $\bar{\epsilon}_1 = -1.95102$, $\delta = \pi/2$. $\beta U_0 = 0.1$, $\beta\epsilon_0 = 0.1$, and $\beta\bar{\mu} = 0.1$, respectively.

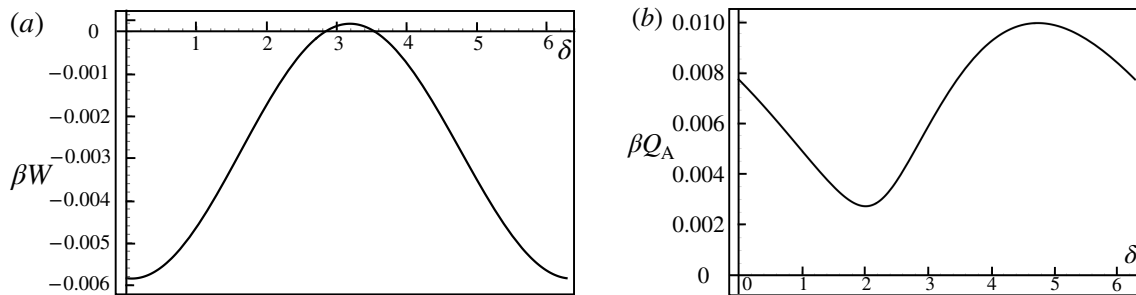


Figure 7. Plots of W (panel (a)) and Q_A (panel (b)) as functions of δ for $r = 0.9$ with $\epsilon/|\bar{\epsilon}_1| = 0.1$, $\bar{\epsilon}_1 = -1.95102$. We set $\beta U_0 = 0.1$, $\beta \epsilon_0 = 0.1$, and $\beta \bar{\mu} = 0.1$.

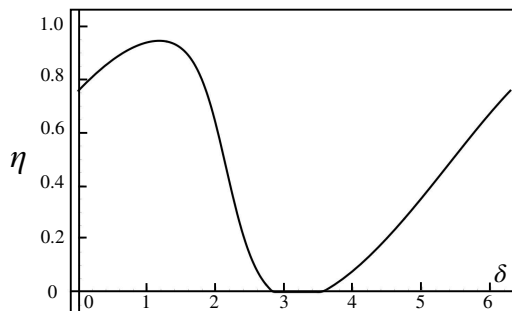


Figure 8. Plot of η against δ for $r = 0.9$ with $\epsilon/|\bar{\epsilon}_1| = 0.1$, $\bar{\epsilon}_1 = -1.95102$. We set $\beta U_0 = 0.1$, $\beta \epsilon_0 = 0.1$, and $\beta \bar{\mu} = 0.1$.

For one-cycle process, we calculate the work and the absorbed heat as functions of δ (Fig. 7). As shown in Fig. 7, βW is negative in a wide region of δ . Thus, we can utilize this system as a thermodynamic engine. Although the sum rule $Q_A - Q_R = -W$ exists, the relationship between the heat absorption or release and W is non-trivial.

From those results, we obtain the efficiency in the present setup as shown in Fig. 8, where the efficiency η is quite high near $\delta \simeq 2\pi/5$. This suggests the potential importance of the application. Note that η is ill-defined if $W > 0$, though we set $\eta = 0$ for this region in Fig. 8.

V. CONCLUDING REMARKS

In this paper, we successfully extended the geometric thermodynamics formulated in Refs. [56–58] to a quantum system coupled to two reservoirs whose electrochemical potentials are slowly modulated. Our engine under periodic modulations corresponds to the Carnot cycle in standard thermodynamics. While our system is an example of adiabatic quantum (Thouless) pumping, the explicit calculation in Sec. III is still quasi-classical. In the adiabatic regime, the work is expressed as the line integral of the vector potential in the parameter space. These results are unchanged from those for the geometric thermodynamic engine obtained in Ref. [58]. We applied the formulation to the Anderson model within the wide-band approximation to obtain the explicit values of one-cycle averaged entropy production, thermodynamic length, adiabatic work, and effective efficiency after the system reaches a geometric (cyclic) state. This is a natural extension of our previous work [64], which analyzed the initial relaxation to reach the geometric state.

So far, we have ignored the cost of manipulating the parameters as in standard thermodynamics. Of course, this assumption is not useful if we consider the possibility of implementing a geometric thermodynamic engine. Although we do not know the correct cost, we evaluate the operation cost by assuming it equals the Joule heat, as discussed in Appendix C. See also Appendix D for obtaining the dynamic and geometric currents. For $\delta \neq 0$, the Joule heat can be estimated as the product of the dynamic current and the electrochemical potential difference. If $\delta = 0$, we may use the Green-Kubo formula to evaluate the conductance, and thus we can estimate the cost. Since our cost evaluation

is far from perfect, we should compare our method with another approach, such as Ref. [77], as our future task.

Our future tasks are as follows: (i) Although we considered the circular modulation of the parameters for simplicity in this study, the optimal path would be determined by the geodesic equation in the curved space characterized by the metric given by the Hessian matrix [78]. We also aim to determine the optimal parameter modulation path for our geometric thermodynamic engine using the geodesic equation. (ii) Because the present method is restricted to the adiabatic case $\epsilon \rightarrow 0$, we need to extend the analysis to the non-adiabatic regime of finite ϵ . References [72, 73] obtained the non-adiabatic solution of a classical master equation and a geometric representation of the non-adiabatic current in a two-level system. We expect to apply these methods to investigate the non-adiabatic effect in heat engines. We also need to consider the entropy production as in Ref. [63] in non-adiabatic processes. (iii) Although we have analyzed a quantum system, our treatment in Sec. III is still quasi-classical. Thus, we have so far been unable to clarify the role of quantum coherence. Brandner and Saito [56] showed that quantum coherence reduces the performance of slowly driven heat engines. On the other hand, it was shown that coherence can enhance the performance of heat engines in Ref. [79, 80]. Therefore, we need to resolve the current confusing situation of whether quantum coherence leads to the enhancement of efficiency by using a fully quantum mechanical model. Furthermore, Viebahn et al. demonstrated that interaction-driven topological pumping cannot be adiabatically connected to non-interacting limits [81]. This may suggest the necessity of exploring quantum coherence effects in our model. On the other hand, Walter et al. observed interaction-induced breakdown of Thouless pumping [82]. This also suggests the importance of quantum coherence effects in adiabatic thermodynamic engines. (iv) We assumed that the master equation (3) is still Markovian even though parameter modulation is present. However, this assumption may not be valid as indicated in Ref. [70]. This is important because the modulation process might become non-CPTP if we use the Markovian dynamics described by Eq. (3). Therefore, we should clarify the effect of non-Markovianity arising from the modulation. (v) Although we considered the reservoirs in our system with continuous spectra, we may extract topological features such as the Chern number if the conduction band is located near energy gaps in the reservoirs. Liu et al. [83] observed disorder-induced topological pumping, suggesting that similar effects could be explored in our model with gapped or disordered reservoirs. This would be an interesting direction for geometric thermodynamics.

ACKNOWLEDGEMENTS

This work is partially supported by JSPS Grant-in-Aid for Scientific Research (KAKENHI Grant No. 25K07156). HH acknowledges the support of the Kyoto University Foundation and the JICA Friendship Program 2.0. The authors acknowledge Ken Funo and Tan Van Vu for their critical reading of this manuscript and useful comments. HH thanks Abhishek Dhar for the indication of Ref. [63].

Appendix A: Eigenvalues and eigenvectors of the Anderson model

In this appendix, we briefly summarize eigenvalues and eigenvectors of the Anderson model. The Anderson model for a quantum dot should have the following four states (corresponding to $n = 4$ in the previous section): doubly occupied, singly occupied with an up-spin, singly occupied with a down-spin, and empty. Therefore, the density matrix should be expressed as a 4×4 matrix. As is shown in Ref. [65], however, the density matrix of the quantum master equation of the Anderson model within the wide-band approximation is reduced to a four-component matrix $\hat{\rho} = \text{diag}[\rho_d, \rho_\uparrow, \rho_\downarrow, \rho_e]$, where ρ_d , ρ_\uparrow , ρ_\downarrow , and ρ_e correspond to probabilities of the doubly occupied state, singly occupied state with up-spin, singly occupied state with down-spin, and empty state, respectively. This means that the model is not fully quantum-mechanical but quasi-classical.

Since $\hat{\rho}$ is diagonal, $|\hat{\rho}\rangle$ also has only four components and the transition matrix $\hat{K}(\mathbf{\Lambda}(\theta))$ in Eq. (3) in the wide band approximation is given by the 4×4 matrix (see Appendix B and Ref. [84] for the derivation)

$$\hat{K}(\mathbf{\Lambda}(\theta)) = \begin{pmatrix} -2f_-^{(1)} & f_+^{(1)} & f_+^{(1)} & 0 \\ f_-^{(1)} & -f_-^{(0)} - f_+^{(1)} & 0 & f_+^{(0)} \\ f_-^{(1)} & 0 & -f_-^{(0)} - f_+^{(1)} & f_+^{(0)} \\ 0 & f_-^{(0)} & f_-^{(0)} & -2f_+^{(0)} \end{pmatrix}, \quad (\text{A1})$$

where we have introduced

$$f_+^{(j)} := f_L^{(j)}(\mu^L, U) + f_R^{(j)}(\mu^R, U) \quad (\text{A2})$$

$$f_-^{(j)} := 2 - \{f_L^{(j)}(\mu^L, U) + f_R^{(j)}(\mu^R, U)\} \quad (\text{A3})$$

with the Fermi distribution

$$f_\alpha^{(j)}(\mu^\alpha(\theta), U(\theta)) := \frac{1}{1 + e^{\beta(\epsilon_\alpha + jU(\theta) - \mu^\alpha(\theta))}} \quad (\text{A4})$$

in the lead $\alpha (= L \text{ or } R)$. Note that Eqs, (A2) and (A3) satisfy the relation

$$f_+^{(j)} + f_-^{(j)} = 2 \quad (\text{A5})$$

for $j = 0$ and 1 .

It is straightforward to obtain the eigenvalues of $K(\mathbf{\Lambda}(\theta))$ in Eq. (A1) as

$$\varepsilon_0 = 0, \quad (\text{A6})$$

$$\varepsilon_1 = -(f_+^{(0)} + f_-^{(1)}), \quad (\text{A7})$$

$$\varepsilon_2 = -(f_-^{(0)} + f_+^{(1)}), \quad (\text{A8})$$

$$\varepsilon_3 = -4. \quad (\text{A9})$$

The left and right eigenvectors corresponding to $\varepsilon_0 = 0$ in Eq. (A6) are given by

$$\langle \ell_0 | = (1, 1, 1, 1), \quad (\text{A10})$$

and

$$|r_0\rangle = \frac{1}{2(f_+^{(0)} + f_-^{(1)})} \begin{pmatrix} f_+^{(0)} f_+^{(1)} \\ f_+^{(0)} f_-^{(1)} \\ f_+^{(0)} f_-^{(1)} \\ f_-^{(0)} f_-^{(1)} \end{pmatrix}, \quad (\text{A11})$$

respectively. Because of Eq. (5) there is the trivial relation $|r_0\rangle = |\hat{\rho}^{\text{ss}}\rangle$ for the diagonal element of the density matrix. Note that $|r_0\rangle$ satisfies $\langle \ell_0 | r_0 \rangle = \text{Tr} \hat{\rho}^{\text{ss}} = 1$. The left and right eigenvectors corresponding to ε_1 in Eq. (A7) are given by

$$\langle \ell_1 | = 2 \left(f_-^{(1)}, \frac{-f_+^{(0)} + f_-^{(1)}}{2}, \frac{-f_+^{(0)} + f_-^{(1)}}{2}, -f_+^{(0)} \right), \quad (\text{A12})$$

and

$$|r_1\rangle = \frac{1}{(f_+^{(0)} + f_-^{(1)})(f_-^{(0)} + f_+^{(1)})} \begin{pmatrix} f_+^{(1)} \\ \frac{-f_+^{(0)} + f_-^{(1)}}{2} \\ \frac{-f_+^{(0)} + f_-^{(1)}}{2} \\ -f_-^{(0)} \end{pmatrix}. \quad (\text{A13})$$

The left and right eigenvectors corresponding to ε_2 in Eq. (A8) are

$$\langle \ell_2 | = 2(0, 1, -1, 0), \quad (\text{A14})$$

and

$$|r_2\rangle = \frac{1}{4} \begin{pmatrix} 0 \\ 1 \\ -1 \\ 0 \end{pmatrix}, \quad (\text{A15})$$

respectively.

The left and right eigenvectors corresponding to ε_2 in Eq. (A9) are

$$\langle \ell_3 | = \left(f_-^{(0)} f_-^{(1)}, -f_-^{(0)} f_+^{(1)}, -f_-^{(0)} f_+^{(1)}, f_+^{(0)} f_+^{(1)} \right), \quad (\text{A16})$$

and

$$|r_3\rangle = \frac{1}{2(f_-^{(0)} + f_+^{(1)})} \begin{pmatrix} 1 \\ -1 \\ -1 \\ 1 \end{pmatrix}. \quad (\text{A17})$$

For the Anderson model, the Hamiltonian in the supervector notation becomes

$$\hat{H} = \begin{pmatrix} 2\epsilon_0 + U & 0 & 0 & 0 \\ 0 & \epsilon_0 & 0 & 0 \\ 0 & 0 & \epsilon_0 & 0 \\ 0 & 0 & 0 & 0 \end{pmatrix}. \quad (\text{A18})$$

In this case, we have the four basis states $|d\rangle, |\uparrow\rangle, |\downarrow\rangle$, and $|e\rangle$ for the system corresponding to the doubly occupied state, the single occupied state with spin up, the single occupied state with spin down, and the empty state, respectively. Thus we have 16 basis in the supervector notation, namely, $\{|d\rangle(d), |d\rangle(\uparrow), \dots, |e\rangle(e)\}$. In the present case, the off-diagonal part is irrelevant and thus we only consider the four basis $\{|d\rangle(d), |\uparrow\rangle(\uparrow), |\downarrow\rangle(\downarrow), |e\rangle(e)\}$. Substituting Eqs. (40) and (A18) into Eq. (25), we obtain $A^2 = 0, A^3 = 0$, and

$$A^1 = \beta U_0 \langle \ell_0 | \begin{pmatrix} 1 & 0 & 0 & 0 \\ 0 & 0 & 0 & 0 \\ 0 & 0 & 0 & 0 \\ 0 & 0 & 0 & 0 \end{pmatrix} |\rho(\phi)\rangle = \beta U_0 \rho_1(\phi), \quad (\text{A19})$$

where $\rho_1(\phi)$ stands for the first component of $|\rho(\phi)\rangle$. The substitution of Eq. (6) into Eq. (A19) yields

$$A^1 = \beta U_0 \left[|r_0(\theta)\rangle + \epsilon \sum_{i=1}^3 C_i(\theta) |r_i(\theta)\rangle \right]. \quad (\text{A20})$$

By using the explicit form of eigenstates given in Eqs. (A11), (A13), (A15), and (A17), we can explicitly write the vector potential as

$$A^1 = \beta U_0 \left[\frac{f_+^{(0)} f_+^{(1)}}{2(f_+^{(0)} + f_+^{(1)})} + \epsilon C_1(\theta) \frac{f_+^{(1)}}{(f_+^{(0)} + f_-^{(1)})(f_-^{(0)} + f_+^{(1)})} + \epsilon C_3(\theta) \frac{1}{2(f_-^{(0)} + f_+^{(1)})} \right]. \quad (\text{A21})$$

As it is expected, the 0th term in ϵ of the vector potential A_{0th}^1 does not contribute to the work generation as $\oint A_{0th}^1 d\lambda = 0$, since it is given by the total derivative of λ as

$$A_{0th}^1 = \beta \frac{\partial}{\partial \lambda} \left[\frac{U + \log \frac{f_+^{(0)} f_+^{(1)}}{f_+^{(0)} + f_+^{(1)}}}{1 + f_+^{(0)}} \right]. \quad (\text{A22})$$

Thus, the vector potential becomes

$$A^1 = \epsilon \beta U_0 \frac{1}{2(f_-^{(0)} + f_+^{(1)})} \left[C_1(\theta) \frac{f_+^{(1)}}{f_+^{(0)} + f_-^{(1)}} + \frac{1}{2} C_3(\theta) \right]. \quad (\text{A23})$$

Appendix B: The derivation of the transition matrix

In this appendix, we present the details of the derivation of the transition matrix which appears in Eq. (3) following Ref. [65]. This appendix consists of two parts. In the first part, we explain the outline of the derivation of the quantum master equation. In the second part, we derive the transition matrix in Eq. (3). The derivations in this appendix are specific to the Anderson model described in Sec. III.

1. Quantum master equation for the Anderson model

In this subsection, we explain the outline of the derivation of the quantum master equation for the Anderson model used in Sec. III. In this part, we use the time t instead of using the phase θ because the system may not relax to a steady state if the time is not long enough. Before moving to the details, we mention that the double-bracket notation is used for the super-vector. The super-vectors in this part correspond to those in the main text as follows.

$$\begin{aligned} |d, d\rangle &= \begin{pmatrix} 1 \\ 0 \\ 0 \\ 0 \end{pmatrix}, \quad |\uparrow, \uparrow\rangle = \begin{pmatrix} 0 \\ 1 \\ 0 \\ 0 \end{pmatrix}, \\ |\downarrow, \downarrow\rangle &= \begin{pmatrix} 0 \\ 0 \\ 1 \\ 0 \end{pmatrix}, \quad |e, e\rangle = \begin{pmatrix} 0 \\ 0 \\ 0 \\ 1 \end{pmatrix}. \end{aligned} \quad (\text{B1})$$

As is assumed, the density matrix of the total system $\hat{\rho}^{\text{tot}}$ is decomposed into the matrix of the system $\hat{\rho}$ and the matrix of the bath in thermal equilibrium $\hat{\rho}^{\text{r}}$ at initial time t_0 ,

$$\hat{\rho}^{\text{tot}}(t_0) = \hat{\rho}(t_0) \otimes \hat{\rho}^{\text{r}}. \quad (\text{B2})$$

The time evolution of $\hat{\rho}^{\text{tot}}(t)$ is described by Liouvillian as

$$\frac{d}{dt}\hat{\rho}^{\text{tot}}(t) = \hat{\mathcal{K}}^{\text{tot}}\hat{\rho}^{\text{tot}}(t). \quad (\text{B3})$$

As is the case of Hamiltonian (37), the Liouvillian $\hat{\mathcal{K}}^{\text{tot}}$ for the total system can be decomposed into $\hat{\mathcal{K}}$, $\hat{\mathcal{K}}^{\text{r}}$, and $\hat{\mathcal{K}}^{\text{int}}$. Let us utilize Dyson's equation for a quantum master equation. By the Laplace transformation of $\hat{\rho}^{\text{tot}}(t)$

$$\hat{\varrho}^{\text{tot}}(z) = \int_{t_0}^{\infty} dt e^{-z(t-t_0)} \hat{\rho}^{\text{tot}}(t), \quad (\text{B4})$$

Eq. (B3) becomes

$$\begin{aligned} \hat{\varrho}^{\text{tot}}(z) &= \frac{1}{z - \hat{\mathcal{K}}^{\text{tot}}} \hat{\rho}(t_0) \\ &= (G^0(z) + G^0(z)\hat{\mathcal{K}}^{\text{int}}G^0(z) + \dots)\hat{\rho}^{\text{tot}}(t_0), \end{aligned} \quad (\text{B5})$$

where $G^0(z) = (z - \hat{\mathcal{K}} - \hat{\mathcal{K}}^{\text{r}})^{-1}$. From Eqs. (B2) and (B5), the reduced density matrix, which is obtained by tracing out the bath degrees of freedom, becomes

$$\hat{\varrho}(z) = \text{Tr}_{\text{r}} \left[\left(G^0(z) + G^0(z)\hat{\mathcal{K}}^{\text{int}}G^0(z)\hat{\mathcal{K}}^{\text{int}}G^0(z) \right) \hat{\rho}(t_0) \otimes \hat{\rho}^{\text{r}} \right], \quad (\text{B6})$$

in the second order of $\hat{\mathcal{K}}^{\text{int}}$. It can be shown that the term is linear in $\hat{\mathcal{K}}^{\text{int}}$ vanishes. By using $\hat{\mathcal{K}}^{\text{r}}\hat{\rho}^{\text{r}} = 0$, the first term of RHS of Eq. (B6) can be rewritten as

$$\text{Tr}_{\text{r}} [G^0(z)\hat{\rho}(t_0) \otimes \hat{\rho}^{\text{r}}] = G_{\text{s}}^0(z)\hat{\rho}(t_0), \quad (\text{B7})$$

where $G_{\text{s}}^0(z) = (z - \hat{\mathcal{K}})^{-1}$. Now we define the effective Liouvillian $\hat{\mathcal{K}}^{\text{eff}}$, which describes the time evolution of $\hat{\rho}$ as

$$\hat{\varrho}(z) = \frac{1}{z - \hat{\mathcal{K}}^{\text{eff}}(z)} \hat{\rho}(t_0). \quad (\text{B8})$$

This is equivalent to the following time evolution equation

$$\frac{d}{dt}\hat{\rho}(t) = \int_{t_0}^t d\tau \hat{\mathcal{K}}^{\text{eff}}(t - \tau)\hat{\rho}(\tau). \quad (\text{B9})$$

Here we can see the non-Markovian memory effect. Using the decomposition of $\hat{\mathcal{K}}^{\text{eff}}(z)$ into the free part $\hat{\mathcal{K}}$ and the self energy part Σ as $\hat{\mathcal{K}}^{\text{eff}} = \hat{\mathcal{K}} + \hat{\Sigma}(z)$, the interaction induces the memory effect. By expanding (B8) in $\mathcal{K}_{\text{eff}}(z)$, we obtain

$$\hat{\rho}(z) = \left(G_s^0(z) + G_s^0(z)\hat{\Sigma}(z)G_s^0(z) + \dots \right) \hat{\rho}(t_0). \quad (\text{B10})$$

From Eqs. (B6), (B7), and (B10), we can easily see that the second order term in Eq. (B6) is equal to second term in Eq. (B10). Thus the lengthy calculation yields [85]

$$\hat{\Sigma}(z) = - \sum_{c,c',\xi=\pm} \sum_{\sigma=\uparrow,\downarrow} cc' J_{-\xi,\sigma}^{c'} |aa'\rangle \langle aa'| J_{\xi,\sigma}^c I(\xi, c, a, a'), \quad (\text{B11})$$

where $|a, b\rangle = |a\rangle\langle b|$ is the two-state vector and $J_{\xi,\uparrow}^c$ is the ladder operators (for the case of \downarrow , the definition is the same) defined as

$$J_{+,\uparrow}^+ = \sum_{a=e,\uparrow,\downarrow,d} (|e, a\rangle\langle\uparrow, a| + |\downarrow, a\rangle\langle d, a|), \quad (\text{B12})$$

$$J_{-,\uparrow}^+ = \sum_{a=e,\uparrow,\downarrow,d} (|\uparrow, a\rangle\langle e, a| + |d, a\rangle\langle\downarrow, a|), \quad (\text{B13})$$

$$J_{+,\uparrow}^- = \sum_{a=e,\uparrow,\downarrow,d} (|a, \uparrow\rangle\langle a, e| + |a, d\rangle\langle a, \downarrow|), \quad (\text{B14})$$

$$J_{-,\uparrow}^- = \sum_{a=e,\uparrow,\downarrow,d} (|a, e\rangle\langle a, \uparrow| + |a, \downarrow\rangle\langle a, d|), \quad (\text{B15})$$

and $I(\xi, c, a, a')$ is given by

$$I = V^2 \sum_k \frac{f^{-\xi c}(\omega_k)}{z + i\xi\omega_k + i\Delta_{a,a'}}, \quad (\text{B16})$$

where $\Delta_{a,a'} := \epsilon_a - \epsilon_{a'}$ is the energy difference between the state a and a' . Here we define $f_L^{-\xi c} + f_R^{-\xi c} = f^{-\xi c}$. In the case of flat band $d\omega_k/dk = \text{const}$, the function I which describes the effect of spectrum in the reservoir on tunneling process, can be rewritten as

$$I = \frac{\Gamma}{\pi} \int_{-D}^D d\omega \frac{f^{-\xi c}(\omega)}{z + i\xi\omega + i\Delta_{a,a'}}, \quad (\text{B17})$$

where the line width Γ is defined as $\Gamma = \pi \mathbf{n} V^2$ with the density of states in reservoirs \mathbf{n} .

Next, we make an assumption that corresponds to neglecting the memory effect in Eq. (B9). This is valid when the time scale of the dynamics is much longer than that of the reservoirs. By taking the long-time limit $z \rightarrow +0$, we can use the Sokhotski-Plemelj relation $\lim_{\eta \rightarrow +0} (\omega + i\eta)^{-1} = -i\pi\delta(\omega) + P\omega^{-1}$. Assuming the wide band limit $D \rightarrow \infty$, the imaginary part of Σ can be negligible and thus, we obtain

$$\hat{\Sigma}(+0) = -\frac{\Gamma}{2} \sum_{c,c',\xi,\sigma} cc' J_{-\xi,\sigma}^{c'} |aa'\rangle \langle aa'| J_{\xi,\sigma}^c f_{\alpha}^{-c\xi} (-\xi\Delta_{aa'}). \quad (\text{B18})$$

By replacing $\hat{\Sigma}(z) \rightarrow \hat{\Sigma}(+0)$ (long-time limit), Eq. (B9) can be rewritten as

$$\frac{d}{dt} \hat{\rho}(t) = \hat{\mathcal{K}}^{\text{eff}}(z = +0) \hat{\rho}(t). \quad (\text{B19})$$

By using this method, we arrive at Eq. (3) by setting $\hat{\mathcal{K}}^{\text{eff}}(z = +0) = 2\pi\Gamma\hat{K}$ and $\theta = 2\pi(t - t_0)/\tau_p$ where t_0 and τ_p are the time to reach the periodic state and the period, respectively.

2. The explicit expression of the transition matrix \hat{K} in Eq. (3) for the Anderson model

As is explained in the previous subsection, the transition matrix $\hat{\mathcal{K}} = \hat{\mathcal{K}}_{\text{eff}}$ is given by

$$\hat{\mathcal{K}} = -\frac{\Gamma}{2} \sum_{c,c',\xi,\sigma} cc' J_{-\xi,\sigma}^{c'} |aa'\rangle \langle aa'| J_{\xi,\sigma}^c f_{\alpha}^{-c\xi} (-\xi\Delta_{aa'}), \quad (\text{B20})$$

where $\alpha = \text{L or R}$, a and a' can take the state of e, \uparrow, \downarrow or d , $c = \pm 1$, $\xi = \pm 1$, and σ is the spin taking the values $\sigma = \uparrow$ and \downarrow . All the subscripts and superscripts are summed up. Here $J_{\xi,\sigma}^c$ is the ladder operator given by Eqs. (B12)-(B15).

a. Calculation for $\langle i, i | \hat{\mathcal{K}} | j, j \rangle$

In this part, we write the result of operation $\hat{\mathcal{K}}$ onto the super-vector $|e, e\rangle$, $|\uparrow, \uparrow\rangle$, $|\downarrow, \downarrow\rangle$, and $|d, d\rangle$ as

$$\hat{\mathcal{K}}|e, e\rangle = -2\Gamma f_+(\epsilon_0)|e, e\rangle + \Gamma f_+(\epsilon_0)|\uparrow, \uparrow\rangle + \Gamma f_+(\epsilon_0)|\downarrow, \downarrow\rangle, \quad (\text{B21})$$

$$\hat{\mathcal{K}}|\uparrow, \uparrow\rangle = \Gamma f_-(\epsilon_0)|e, e\rangle + \Gamma f_+(\epsilon_0 + U)|d, d\rangle - \Gamma[f_-(\epsilon_0) + f_+(\epsilon_0 + U)]|\uparrow, \uparrow\rangle, \quad (\text{B22})$$

$$\hat{\mathcal{K}}|\downarrow, \downarrow\rangle = \Gamma f_-(\epsilon_0)|e, e\rangle + \Gamma f_+(\epsilon_0 + U)|d, d\rangle - \Gamma[f_-(\epsilon_0) + f_+(\epsilon_0 + U)]|\downarrow, \downarrow\rangle, \quad (\text{B23})$$

$$\hat{\mathcal{K}}|d, d\rangle = -2\Gamma f_-(\epsilon_0 + U)|d, d\rangle + \Gamma f_-(\epsilon_0 + U)|\uparrow, \uparrow\rangle + \Gamma f_-(\epsilon_0 + U)|\downarrow, \downarrow\rangle, \quad (\text{B24})$$

where we use $\Delta_{a, a'} = -\Delta_{a', a} = \epsilon_0$. These results yield each component of K-matrix as follows:

$$\begin{aligned} & \begin{pmatrix} \langle d, d | \hat{\mathcal{K}} | d, d \rangle & \langle d, d | \hat{\mathcal{K}} | \uparrow, \uparrow \rangle & \langle d, d | \hat{\mathcal{K}} | \downarrow, \downarrow \rangle & \langle d, d | \hat{\mathcal{K}} | e, e \rangle \\ \langle \uparrow, \uparrow | \hat{\mathcal{K}} | d, d \rangle & \langle \uparrow, \uparrow | \hat{\mathcal{K}} | \uparrow, \uparrow \rangle & \langle \uparrow, \uparrow | \hat{\mathcal{K}} | \downarrow, \downarrow \rangle & \langle \uparrow, \uparrow | \hat{\mathcal{K}} | e, e \rangle \\ \langle \downarrow, \downarrow | \hat{\mathcal{K}} | d, d \rangle & \langle \downarrow, \downarrow | \hat{\mathcal{K}} | \uparrow, \uparrow \rangle & \langle \downarrow, \downarrow | \hat{\mathcal{K}} | \downarrow, \downarrow \rangle & \langle \downarrow, \downarrow | \hat{\mathcal{K}} | e, e \rangle \\ \langle e, e | \hat{\mathcal{K}} | d, d \rangle & \langle e, e | \hat{\mathcal{K}} | \uparrow, \uparrow \rangle & \langle e, e | \hat{\mathcal{K}} | \downarrow, \downarrow \rangle & \langle e, e | \hat{\mathcal{K}} | e, e \rangle \end{pmatrix} \\ &= \Gamma \begin{pmatrix} -2f_-(\epsilon_0 + U) & f_+(\epsilon_0 + U) & f_+(\epsilon_0 + U) & 0 \\ f_-(\epsilon_0 + U) & -f_-(\epsilon_0) - f_+(\epsilon_0 + U) & 0 & f_+(\epsilon_0) \\ f_-(\epsilon_0 + U) & 0 & -f_-(\epsilon_0) - f_+(\epsilon_0 + U) & f_+(\epsilon_0) \\ 0 & f_-(\epsilon_0) & f_-(\epsilon_0) & -2f_+(\epsilon_0) \end{pmatrix} \\ &= \Gamma \begin{pmatrix} -2f_-^{(1)} & f_+^{(1)} & f_+^{(1)} & 0 \\ f_-^{(1)} & -f_-^{(0)} - f_+^{(1)} & 0 & f_+^{(0)} \\ f_-^{(1)} & 0 & -f_-^{(0)} - f_+^{(1)} & f_+^{(0)} \\ 0 & f_-^{(0)} & f_-^{(0)} & -2f_+^{(0)} \end{pmatrix}. \end{aligned} \quad (\text{B25})$$

This is identical to Eq. (A1).

Appendix C: Cost for parameter modulation

The nonequilibrium system is sustained by an external agent, which incurs a cost. However, the main text ignores such a cost. In this appendix, we evaluate the cost associated with modulating parameters in our system.

The dominant cost modulating the parameters should compensate for the Joule heating over a single cycle. If there exists a chemical potential difference between two reservoirs, the Joule heat can be evaluated as the product of the dynamic current and the chemical potential difference. We present this result in Appendix C 1. However, this naive approach cannot be used for $\delta = 0$ in the absence of the chemical potential difference. Even in this case, there should be costs to modulate systems. In this case, we propose an alternative method to evaluate the Joule heating caused by the geometric current with the aid of the Green-Kubo formula, as shown in Appendix C 2.

1. Joule heat by dynamic current

If there exists a chemical potential difference between two reservoirs (bias voltage), a dynamic current exists. Thus, the cost to maintain the driven system can be estimated solely by the Joule heat of the dynamic current multiplied by the bias voltage.

The energy transfer is associated with the transfer of electric current. For Joule heating, the electron transfer always gives positive contributions irrespective of the direction of the flow. In this case, the Joule heating rate is expected to be proportional to the current and the bias voltage between the reservoirs L and R . Here, we use $V_{\text{bi}, \alpha}^{(j)} := \mu_{L/R} - (\epsilon_0 + jU)$ as the bias voltage between the quantum dot and the reservoir $\alpha = L$ or R , where $j = 0$ and $j = 1$ correspond to the empty state and the occupied state, respectively. We define $V_{\text{bi}, L/R}^{(0)}$ as the bias voltage for the empty state and $V_{\text{bi}, L/R}^{(1)}$ for the occupied state, accounting for the occupation-dependent energy level in the quantum dot. Although the Joule heat rate \dot{q}^J generated in the unit time is given by the product of the total current and the bias voltage, we can ignore the contribution of the geometric current if the dynamic current exists. Thus, we

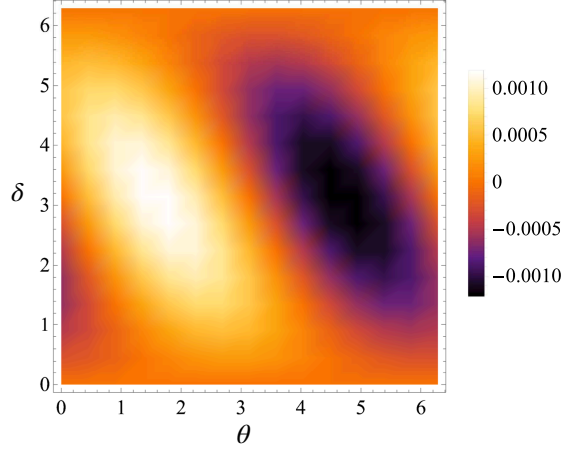


Figure 9. Plot of the dynamic current $J_{R,d}(\theta, \delta)$, where we set $\beta\epsilon_0 = 0.1, \beta\bar{\mu} = 0.1, \beta U_0 = 0.1, r = 0.9$, and $\epsilon/|\bar{\epsilon}_1| = 0.1, \bar{\epsilon}_1 = -1.95102$.

obtain

$$\dot{q}^J(\theta, \delta) := \sum_{\alpha=L,R} \sum_{j=0,1} V_{\text{bi},\alpha}^{(j)} J_{\alpha,d}^{(j)}(\theta, \delta), \quad (\text{C1})$$

where $J_{\alpha,d}^{(0)}$ and $J_{\alpha,d}^{(1)}$ are the dynamic currents in the lead α emitted from the empty state and the occupied state in the QD, respectively. Note that the dynamic current $J_{\alpha,d}^{(j)}$ with $j = 0$ or 1 can be calculated in terms of the counting field as shown in Appendix D. We also note that if the charge accumulation in the quantum is absent, $J_{L,d}^{(j)} = -J_{R,d}^{(j)}$ is satisfied and Eq. (C1) reduces to the usual form of the Joule heat $(\mu_R - \mu_L)(J_{R,d}^{(0)} + J_{R,d}^{(1)})$.

In Fig. 9, we plot the dynamic current as a function of δ and θ with $\beta\epsilon_0 = 0.1, \beta\bar{\mu} = 0.1, \beta U_0 = 0.1, \epsilon/|\bar{\epsilon}_1| = 0.1$ and $r = 0.9$. As can be seen, a pair of positive and negative peaks exists in the parameter space.

The Joule heat generated in the single cycle for $\delta \neq 0$ is given by

$$q^J(\delta) := \int_{\theta_{\text{in}}}^{2\pi+\theta_{\text{in}}} d\theta \dot{q}^J(\theta, \delta). \quad (\text{C2})$$

We note that this evaluation is rather phenomenological.

In Fig. 10, we plot $\dot{q}^J(\theta, \delta)$ as functions of θ and δ for $\beta\epsilon_0 = 0.1, \beta\bar{\mu} = 0.1, \beta U_0 = 0.1, \epsilon/|\bar{\epsilon}_1| = 0.1, \bar{\epsilon}_1 = -1.95102, \theta_{\text{in}} = 2\pi$, and $r = 0.9$. It shows that the Joule heat is positive and depends on δ and θ . This heat is dissipated into the environment and corresponds to the cost of maintaining this engine.

By considering the cost of modulating the system, we can define the alternative efficiency $\tilde{\eta}$ in the region of $\mathcal{W} < 0$ as

$$\tilde{\eta} := \frac{|W|}{Q_A + q^J(\delta)}. \quad (\text{C3})$$

In Fig. 11, we plot $\tilde{\eta}$ against δ with $\beta\epsilon_0 = 0.1, \beta\bar{\mu} = 0.1, \beta U_0 = 0.1, \epsilon/|\bar{\epsilon}_1| = 0.1, \bar{\epsilon}_1 = -1.95102$ and $r = 0.9$. The result shows that the efficiency $\tilde{\eta}$ becomes much smaller than η without consideration of the cost. However, in the low bias region (near $\theta = 0, 2\pi$), $\tilde{\eta}$ is still high since the dynamic current is small.

2. Green-Kubo Formula

So far, we have considered the Joule heat generated by the dynamic current and bias voltage. However, such a Joule heat becomes zero if we consider the zero bias case $\delta = 0$. We do not think that the operation cost is zero in this situation. For this purpose, we adopt the Green-Kubo formula to evaluate the conductance, the inverse of the resistance. Then, the product of the resistance and the geometric current can be regarded as the Joule heat.

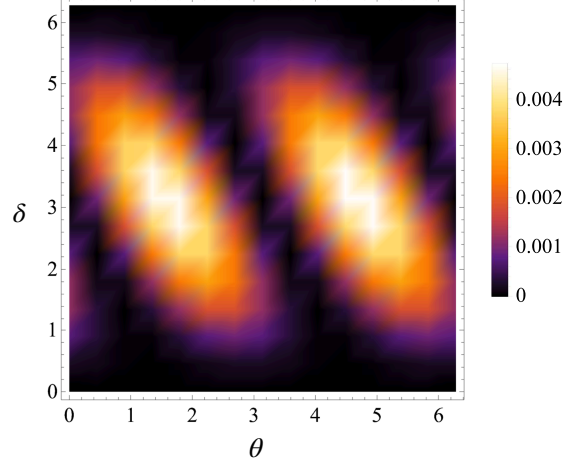


Figure 10. Plot of the Joule heat generated in the unit time $q^J(\theta, \delta)$ as functions of θ and δ , where we set $\beta\epsilon_0 = 0.1$, $\beta\bar{\mu} = 0.1$, $\beta U_0 = 0.1$, $\epsilon/|\bar{\epsilon}_1| = 0.1$ and $r = 0.9$.

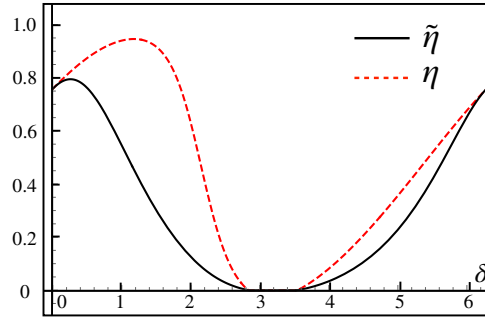


Figure 11. Plot of the efficiency $\tilde{\eta}$ (solid line) with the cost. We set $\beta\epsilon_0 = 0.1$, $\beta\bar{\mu} = 0.1$, $\beta U_0 = 0.1$, $r = 0.9$, and $\epsilon/|\bar{\epsilon}_1| = 0.1$, $\bar{\epsilon}_1 = -1.95102$. For comparison, we recast the efficiency η without the cost (dashed line) already presented in the main text.

Let us consider the dimensionless conductance defined by the Green-Kubo formula:

$$\sigma := \beta^2 \int_{\theta_{\text{in}}}^{2\pi+\theta_{\text{in}}} e^{i\delta\theta} \langle \Delta J(\theta) \Delta J(\theta_{\text{in}}) \rangle d\theta = \beta^2 \int_0^{2\pi} d\delta \theta e^{i\delta\theta} \langle \delta J(\delta\theta) \delta J(0) \rangle. \quad (\text{C4})$$

where $\langle \cdot \rangle := \text{Tr}(\rho(\theta_{\text{in}}) \cdot)$, $\delta\theta := \theta - \theta_{\text{in}}$ and $\Delta J(\theta) := J(\theta) - \bar{J}$ with the electric current $J(\theta)$ and the averaged current \bar{J} defined as $\bar{J} := \frac{1}{2\pi} \int_{\theta_{\text{in}}}^{2\pi+\theta_{\text{in}}} J(\theta) d\theta$. Here, $\delta J(\delta\theta)$ is equivalent to $\Delta J(\theta - \theta_{\text{in}})$. Note that $J(\theta)$ consists of the dynamic current and the geometric current, namely $J(\theta) = J_d(\theta) + J_g(\theta)$. Since we consider the dynamics under the periodic modulation of the parameter after reaching a geometric state (quasi-steady oscillated state), $\langle \delta J(\theta) \delta J(0) \rangle$ is periodic in θ with the periodicity 2π . σ is about 4.482×10^{-6} for $\delta = 0$, $\beta\epsilon_0 = 0.1$, $\beta\bar{\mu} = 0.1$, $\beta U_0 = 0.1$, $\epsilon/|\bar{\epsilon}_1| = 0.1$, $\bar{\epsilon}_1 = -1.95102$ and $r = 0.9$ where the dynamic current disappears. In this case, the Joule heat may be evaluated as $q_{\text{GK}} := \bar{J}_g^2 / \sigma \approx 1.24936$, which results in the efficiency $\eta_{\text{GK}} := |W| / (Q_A + q_{\text{GK}})$ to be $\eta_{\text{GK}} \approx 0.00988114$, where $\bar{J}_g^2 := \int_{\theta_{\text{in}}}^{2\pi+\theta_{\text{in}}} J_g(\theta)^2 d\theta$. As expected, this value is quite low. Therefore, we conclude that the cost of the modulation is dominant.

Appendix D: Counting field and current

In this appendix, we explain the method to obtain the current generated during the parameter modulation. The current under a cyclic modulation consists of two parts. One is the dynamic current, and the other is the geometric current.

As in Refs. [32, 39], we introduce a set of counting fields $\boldsymbol{\chi}$ to calculate physical observables. First, we consider the dynamic current. As a result, Eq. (3) is formally modified as

$$\frac{d}{d\theta} |\hat{\rho}(\theta, \delta, \boldsymbol{\chi})\rangle = \epsilon^{-1} \hat{K}^{\boldsymbol{\chi}} |\hat{\rho}(\theta, \delta, \boldsymbol{\chi})\rangle, \quad (\text{D1})$$

where the set of counting fields contains two components $\boldsymbol{\chi} = (\chi_L, \chi_R)$, which are inserted to monitor the time evolution of the housekeeping entropy production in the left and right lead, respectively, and $|\hat{\rho}(\theta, \delta, \boldsymbol{\chi})\rangle$ and $\hat{K}^{\boldsymbol{\chi}}$ are the generalized density matrix and the evolution operator, respectively. Since $\hat{\rho}(\theta, \delta, \boldsymbol{\chi})$ behaves as $\hat{\rho}(\theta, \delta, \boldsymbol{\chi}) \sim \exp[\lambda_0(\boldsymbol{\Lambda}, \boldsymbol{\chi})\theta/\epsilon]$ for large θ/ϵ with the smallest eigenvalue $\lambda_0(\boldsymbol{\Lambda}, \boldsymbol{\chi})$ of $\hat{K}^{\boldsymbol{\chi}}$ (which is reduced to zero in the limit $\boldsymbol{\chi} \rightarrow \mathbf{0}$) under a fixed $\boldsymbol{\Lambda}$, the current is given by

$$J_\alpha(\phi, \delta) := \left. \frac{\partial \lambda_0(\boldsymbol{\Lambda}(\phi, \delta), \boldsymbol{\chi})}{\partial (i\chi_\alpha)} \right|_{\boldsymbol{\chi}=\mathbf{0}}. \quad (\text{D2})$$

Note that χ_L and χ_R couple to the number operators of the electrons in the left reservoir (\hat{N}_L) and that in the right reservoir (\hat{N}_R), respectively, where \hat{N}_α ($\alpha = L, R$) stands for the number operator of the reservoir α . In the absence of the Hamiltonian's modulation in the system, we obtain $J_L = -J_R$ due to the current conservation, while this relation does not hold if the charge population in the system can be changed. These currents result in Joule heating.

The operator $\hat{K}^{\boldsymbol{\chi}}$ in Eq. (D1) can be expressed as

$$\hat{K}^{\boldsymbol{\chi}} = \hat{K} + i \sum_{\alpha=L,R} \chi_\alpha \hat{\mathcal{K}}_\alpha + O(\chi^2). \quad (\text{D3})$$

To explicitly compute Eq. (D2), we utilize the Anderson model. We define the generating function as

$$\ln \text{Tr} \rho(\theta, \delta, \boldsymbol{\chi}) = \ln \left\langle e^{i(\chi_L \hat{N}_L(\theta) + \chi_R \hat{N}_R(\theta, \delta))} \right\rangle, \quad (\text{D4})$$

where the angle brackets denote thermal and quantum averages. In this context, only the interaction Hamiltonian \hat{H}^{int} in the total Hamiltonian does not commute with $e^{i(\chi_L \hat{N}_L + \chi_R \hat{N}_R)}$. Consequently, we adopt the technique described in Ref. [65], whereby counting fields are incorporated as phases in the interaction Hamiltonian:

$$e^{-i\frac{\chi}{2}\hat{N}_\alpha} V_\beta d_\sigma^\dagger a_{\beta,k,\sigma} e^{i\frac{\chi}{2}\hat{N}_\alpha} = e^{i\frac{\chi}{2}\delta_{\alpha\beta}} V_\beta d_\sigma^\dagger a_{\beta,k,\sigma}, \quad (\text{D5})$$

$$e^{-i\frac{\chi}{2}\hat{N}_\alpha} V_\beta a_{\beta,k,\sigma}^\dagger d_\sigma e^{i\frac{\chi}{2}\hat{N}_\alpha} = e^{i\frac{\chi}{2}\delta_{\alpha\beta}} V_\beta a_{\beta,k,\sigma}^\dagger d_\sigma. \quad (\text{D6})$$

Then, we proceed with the following transposition to calculate the generating function.

$$a_{\alpha,k,\sigma}^\dagger \rightarrow e^{i\frac{\chi_\alpha}{2}} a_{\alpha,k,\sigma}^\dagger, \quad (\text{D7})$$

$$a_{\alpha,k,\sigma} \rightarrow e^{-i\frac{\chi_\alpha}{2}} a_{\alpha,k,\sigma}. \quad (\text{D8})$$

As a consequence, the similar calculation in Ref. [65] yields $\hat{K}^{\boldsymbol{\chi}}$ as

$$\hat{K}^{\boldsymbol{\chi}} = \Gamma \begin{pmatrix} -2f_-^{(1)\boldsymbol{\chi}} & f_+^{(1)\boldsymbol{\chi}} & f_+^{(1)\boldsymbol{\chi}} & 0 \\ f_-^{(1)\boldsymbol{\chi}} & -f_+^{(0)} - f_+^{(1)} & 0 & f_+^{(0)\boldsymbol{\chi}} \\ f_-^{(1)\boldsymbol{\chi}} & 0 & -f_+^{(0)} - f_+^{(1)} & f_+^{(0)\boldsymbol{\chi}} \\ 0 & f_-^{(0)\boldsymbol{\chi}} & f_-^{(0)\boldsymbol{\chi}} & -2f_+^{(0)} \end{pmatrix}, \quad (\text{D9})$$

where $f_+^{(j)\boldsymbol{\chi}} = e^{i\chi_L} f_L^{(j)}(\epsilon_0) + e^{i\chi_R} f_R^{(j)}(\epsilon_0)$ and $f_-^{(j)\boldsymbol{\chi}} = e^{-i\chi_L} [1 - f_L^{(j)}(\epsilon_0)] + e^{-i\chi_R} [1 - f_R^{(j)}(\epsilon_0)]$. Here, $f_\alpha^{(j)}(\epsilon_0) = [1 + e^{\beta(\epsilon_0 + jU - \mu_\alpha)}]^{-1}$ corresponds to the Fermi distribution function. Substituting Eq. (D9) into Eq. (D3), we can write $\hat{\mathcal{K}}_\alpha$ as

$$\hat{\mathcal{K}}_\alpha = \begin{pmatrix} 0 & g_\alpha^1 & g_\alpha^1 & 0 \\ g_\alpha^1 - 1 & 0 & 0 & g_\alpha^0 \\ g_\alpha^1 - 1 & 0 & 0 & g_\alpha^0 \\ 0 & g_\alpha^0 - 1 & g_\alpha^0 - 1 & 0 \end{pmatrix}, \quad (\text{D10})$$

with $g_\alpha^j := (1 + e^{\beta(\epsilon_0 + jU - \mu_\alpha)})^{-1}$ ($j = 1, 2$, $\alpha = L, R$). For the later convenience, we further decompose (D10) into the transfer matrices $\hat{\mathcal{K}}_\alpha^{(0)}$ and $\hat{\mathcal{K}}_\alpha^{(1)}$ as

$$\hat{\mathcal{K}}_\alpha = \hat{\mathcal{K}}_\alpha^{(0)} + \hat{\mathcal{K}}_\alpha^{(1)}, \quad (\text{D11})$$

where

$$\hat{\mathcal{K}}_\alpha^{(0)} = \begin{pmatrix} 0 & 0 & 0 & 0 \\ 0 & 0 & 0 & g_\alpha^0 \\ 0 & 0 & 0 & g_\alpha^0 \\ 0 & g_\alpha^0 - 1 & g_\alpha^0 - 1 & 0 \end{pmatrix}, \quad (\text{D12})$$

$$\hat{\mathcal{K}}_\alpha^{(1)} = \begin{pmatrix} 0 & g_\alpha^1 & g_\alpha^1 & 0 \\ g_\alpha^1 - 1 & 0 & 0 & 0 \\ g_\alpha^1 - 1 & 0 & 0 & 0 \\ 0 & 0 & 0 & 0 \end{pmatrix}, \quad (\text{D13})$$

Here $\hat{\mathcal{K}}_\alpha^{(0)}$ ($\hat{\mathcal{K}}_\alpha^{(1)}$) denotes the processes that change the state in the quantum dot from the empty state to the singly occupied state (from the singly occupied state to the doubly occupied state) and vice versa. Using the relation

$$\tilde{\lambda}_{0,\alpha}(\mathbf{\Lambda}(\phi, \delta)) = \langle \ell_0 | \hat{\mathcal{K}}_\alpha(\mathbf{\Lambda}(\phi, \delta)) | r_0 \rangle. \quad (\text{D14})$$

and the expansion

$$\lambda_0(\mathbf{\Lambda}(\phi, \delta), \boldsymbol{\chi}) = i \sum_\alpha \chi_\alpha \tilde{\lambda}_{0,\alpha}(\mathbf{\Lambda}(\phi, \delta)) + O(\chi^2), \quad (\text{D15})$$

we obtain $\lambda_0(\mathbf{\Lambda}, \boldsymbol{\chi})$ and $J_{\alpha,d}$.

By the straightforward calculation, we obtain

$$\begin{aligned} J_{\alpha,d} &= \tilde{\lambda}_{0,\alpha}(\mathbf{\Lambda}(\phi, \delta)) \\ &= \frac{1}{f_-^{(1)} + f_+^{(0)}} \left[f_-^{(0)} f_-^{(1)} g_\alpha^0 + (g_\alpha^0 + g_\alpha^1 - 1) f_+^{(0)} f_-^{(1)} + f_+^{(0)} f_+^{(1)} (g_\alpha^1 - 1) \right], \end{aligned} \quad (\text{D16})$$

where the currents are defined to be positive if currents flow from the quantum dot to the reservoirs. Here, J_L and J_R are defined as positive if the electrons come into the quantum dot and negative if the electrons go out from the quantum dot. We set $\beta\epsilon_0 = 0.1$, $\beta\mu = 0.1$, $\beta U_0 = 0.1$, and $r = 0.9$. By using decomposition (D11), this dynamic current can be further decomposed as

$$J_{\alpha,d} = J_{\alpha,d}^{(0)} + J_{\alpha,d}^{(1)}, \quad (\text{D17})$$

$$J_{\alpha,d}^{(0)} = \frac{1}{f_-^{(1)} + f_+^{(0)}} \left[f_-^{(0)} f_-^{(1)} g_\alpha^0 + (g_\alpha^0 - 1) f_+^{(0)} f_-^{(1)} \right], \quad (\text{D18})$$

$$J_{\alpha,d}^{(1)} = \frac{1}{f_-^{(1)} + f_+^{(0)}} \left[g_\alpha^1 f_-^{(1)} f_+^{(0)} + (g_\alpha^1 - 1) f_+^{(0)} f_+^{(1)} \right]. \quad (\text{D19})$$

The geometric current can also be calculated by using a counting field. The excess charge transfer during one cycle becomes

$$\Delta Q_{\text{ex}} := - \int_{\theta_{\text{in}}}^{2\pi + \theta_{\text{in}}} \frac{\partial \langle \ell_0 |}{\partial i\chi} \Big|_{\chi=0} \cdot \frac{d|r_0\rangle}{d\theta} d\theta. \quad (\text{D20})$$

Thus, the geometric current J_g is defined as

$$J_g := \frac{1}{\tau_p} \Delta Q_{\text{ex}} = - \frac{1}{\tau_p} \int_{\theta_{\text{in}}}^{2\pi + \theta_{\text{in}}} \frac{\partial \langle \ell_0 |}{\partial i\chi} \Big|_{\chi=0} \cdot \frac{d|r_0\rangle}{d\theta} d\theta. \quad (\text{D21})$$

For later convenience, we introduce the instantaneous geometric current $j_g(t)$ as

$$j_g := - \frac{1}{2\pi} \frac{\partial \langle \ell_0 |}{\partial i\chi} \Big|_{\chi=0} \cdot \frac{d|r_0\rangle}{d\theta}. \quad (\text{D22})$$

-
- [1] D. J. Thouless, Quantization of particle transport, *Phys. Rev. B* **27**, 6083 (1983).
- [2] Q. Niu and D. J. Thouless, Quantised adiabatic charge transport in the presence of substrate disorder and many-body interaction, *J. Phys. A : Math. Gen.* **17**, 2453 (1984).
- [3] M. V. Berry, Quantal phase factors accompanying adiabatic changes, *Proc. R. Soc. London Ser. A* **392**, 45 (1984).
- [4] D. Xiao, M.-C. Chang, and Q. Niu, Berry phase effects on electronic properties, *Rev. Mod. Phys.* **82**, 1959 (2010).
- [5] N. A. Sinitsyn and I. Nemenman, The Berry phase and the pump flux in stochastic chemical kinetics, *EPL* **77**, 58001 (2007).
- [6] N. A. Sinitsyn and I. Nemenman, Universal Geometric Theory of Mesoscopic Stochastic Pumps and Reversible Ratchets, *Phys. Rev. Lett.* **99**, 220408 (2007).
- [7] L. P. Kouwenhoven, A. T. Johnson, N. C. van der Vaart, C. J. P. M. Harmans, and C. T. Foxon, Quantized current in a quantum-dot turnstile using oscillating tunnel barriers, *Phys. Rev. Lett.* **67**, 1626 (1991).
- [8] H. Pothier, P. Lafarge, C. Urbina, D. Esteve, and M. H. Devoret, Single-Electron Pump Based on Charging Effects, *Europhys. Lett.* **17**, 249 (1992).
- [9] M. Switkes, C. M. Marcus, K. Campman, and A. C. Gossard, An Adiabatic Quantum Electron Pump, *Science* **283**, 1905 (1999).
- [10] A. Fuhrer, C. Fasth, and L. Samuelson, Single electron pumping in InAs nanowire double quantum dots, *Appl. Phys. Lett.* **91**, 052109 (2007).
- [11] B. Kaestner, V. Kashcheyevs, G. Hein, K. Pierz, U. Siegner, and H. W. Schumacher, Robust single-parameter quantized charge pumping, *Appl. Phys. Lett.* **92**, 192106 (2008).
- [12] S. J. Chorley, J. Frake, C. G. Smith, G. A. C. Jones, and M. R. Buitelaar, Quantized charge pumping through a carbon nanotube double quantum dot, *Appl. Phys. Lett.* **100**, 143104 (2012).
- [13] S. Nakajima, T. Tomita, S. Taie, T. Ichinose, H. Ozawa, L. Wang, M. Troyer and Y. Takahashi, Topological Thouless pumping of ultracold fermions, *Nature Physics* **12**, 296 (2016).
- [14] M. Lohse, C. Schweizer, O. Zilberberg, M. Aidelsburger and I. Bloch, A Thouless quantum pump with ultracold bosonic atoms in an optical superlattice, *Nature Physics* **12**, 350 (2016).
- [15] S. K. Watson, R. M. Potok, C. M. Marcus, and V. Umansky, Experimental Realization of a Quantum Spin Pump, *Phys. Rev. Lett.* **91**, 258301 (2003).
- [16] P. W. Brouwer, Scattering approach to parametric pumping, *Phys. Rev. B* **58**, R10135 (1998).
- [17] J. E. Avron, A. Elgart, G. M. Graf, and L. Sadun, Geometry, statistics, and asymptotics of quantum pumps, *Phys. Rev. B* **62**, R10618 (2000).
- [18] M. Moskalets and M. Büttiker, Effect of inelastic scattering on parametric pumping, *Phys. Rev. B* **64**, 201305(R) (2001).
- [19] J. N. H. J. Cremers and P. W. Brouwer, Dephasing in a quantum pump, *Phys. Rev. B* **65**, 115333 (2002).
- [20] A. Andreev and A. Kamenev, Counting Statistics of an Adiabatic Pump, *Phys. Rev. Lett.* **85**, 1294 (2000).
- [21] Y. Makhlin and A. D. Mirlin, Counting Statistics for Arbitrary Cycles in Quantum Pumps, *Phys. Rev. Lett.* **87**, 276803 (2001).
- [22] I. L. Aleiner and A. V. Andreev, Adiabatic Charge Pumping in Almost Open Dots, *Phys. Rev. Lett.* **81**, 1286 (1998).
- [23] E. R. Mucciolo, C. Chamon, and C. M. Marcus, Adiabatic Quantum Pump of Spin-Polarized Current, *Phys. Rev. Lett.* **89**, 146802 (2002).
- [24] J. M. R. Parrondo, Reversible ratchets as Brownian particles in an adiabatically changing periodic potential, *Phys. Rev. E* **57**, 7297 (1998).
- [25] O. Usmani, E. Lutz, and M. Büttiker, Noise-assisted classical adiabatic pumping in a symmetric periodic potential, *Phys. Rev. E* **66**, 021111 (2002).
- [26] R. D. Astumian, Adiabatic Pumping Mechanism for Ion Motive ATPases, *Phys. Rev. Lett.* **91**, 118102 (2003).
- [27] R. D. Astumian, Adiabatic operation of a molecular machine, *Proc. Natl. Acad. Sci. USA* **104**, 19715 (2007).
- [28] S. Rahav, J. Horowitz, and C. Jarzynski, Directed Flow in Nonadiabatic Stochastic Pumps, *Phys. Rev. Lett.* **101**, 140602 (2008).
- [29] V. Y. Chernyak, J. R. Klein, and N. A. Sinitsyn, Quantization and fractional quantization of currents in periodically driven stochastic systems. I. Average currents, *J. Chem. Phys.* **136**, 154107 (2012).
- [30] V. Y. Chernyak, J. R. Klein, and N. A. Sinitsyn, Quantization and fractional quantization of currents in periodically driven stochastic systems. II. Full counting statistics, *J. Chem. Phys.* **136**, 154108 (2012).
- [31] J. Ren, P. Hänggi, and B. Li, Berry-Phase-Induced Heat Pumping and Its Impact on the Fluctuation Theorem, *Phys. Rev. Lett.* **104**, 170601 (2010).
- [32] T. Sagawa and H. Hayakawa, Geometric expression of excess entropy production, *Phys. Rev. E* **84**, 051110 (2011).
- [33] V. M. M. Paasonen and H. Hayakawa, Pumping current in a non-Markovian N-state model *Phys. Rev. Research* **3**, 023238 (2021).
- [34] F. Renzoni and T. Brandes, Charge transport through quantum dots via time-varying tunnel coupling, *Phys. Rev. B* **64**, 245301 (2001).
- [35] T. Brandes and T. Vorrath, Adiabatic transfer of electrons in coupled quantum dots, *Phys. Rev. B* **66**, 075341 (2002).
- [36] E. Cota, R. Aguado, and G. Platero, ac-Driven Double Quantum Dots as Spin Pumps and Spin Filters, *Phys. Rev. Lett.* **94**, 107202 (2005).
- [37] J. Splettstoesser, M. Governale, J. König, and R. Fazio, Adiabatic pumping through a quantum dot with coulomb inter-

- actions: A perturbation expansion in the tunnel coupling, *Phys. Rev. B* **74**, 085305 (2006).
- [38] T. Yuge, T. Sagawa, A. Sugita, and H. Hayakawa, Geometric pumping in quantum transport: Quantum master equation approach, *Phys. Rev. B* **86**, 235308 (2012).
- [39] T. Yuge, T. Sagawa, A. Sugiura, and H. Hayakawa, Geometric Excess Entropy Production in Nonequilibrium Quantum Systems, *J. Stat. Phys.* **153**, 412 (2013).
- [40] K. L. Watanabe and H. Hayakawa, Geometric fluctuation theorem for a spin-boson system, *Phys. Rev. E* **96**, 022118 (2017).
- [41] Y. Hino and H. Hayakawa, Fluctuation relations for adiabatic pumping, *Phys. Rev. E* **120**, 012115 (2020).
- [42] K. Takahashi, Y. Hino, K. Fujii, and H. Hayakawa, Full Counting Statistics and Fluctuation-Dissipation Relation for Periodically Driven Two-State Systems, *J. Stat. Phys.* **181**, 2206 (2020).
- [43] B. Andresen, Finite-time thermodynamics and thermodynamic length, *Rev. Gén. Therm.* **35**, 647 (1996).
- [44] F. Weinhold, Metric geometry of equilibrium thermodynamics, *J. Chem. Phys.* **63**, 2479 (1975).
- [45] G. Ruppeiner, Thermodynamics: A Riemannian geometric model, *Phys. Rev. A* **20**, 1608 (1979).
- [46] P. Salamon and R. S. Berry, Thermodynamic Length and Dissipated Availability, *Phys. Rev. Lett.* **51**, 1127 (1983).
- [47] F. Schlögl, Thermodynamic metric and stochastic measures, *Z. Phys. B* **59**, 449 (1985).
- [48] G. Ruppeiner, Riemannian geometry in thermodynamic fluctuation theory, *Rev. Mod. Phys.* **67**, 605 (1995).
- [49] G. E. Crooks, Measuring Thermodynamic Length, *Phys. Rev. Lett.* **99**, 100602 (2007).
- [50] S. Deffner and E. Lutz, Thermodynamic length for far-from-equilibrium quantum systems, *Phys. Rev. E* **87**, 022143 (2013).
- [51] M. Scandi and M. Perarnau-Llobet, Thermodynamic length in open quantum systems, *Quantum* **3**, 197 (2019).
- [52] P. Hänggi and F. Marchesoni, Artificial Brownian motors: Controlling transport on the nanoscale, *Rev. Mod. Phys.* **81**, 387 (2009).
- [53] J. Gemmer, M. Michel, and G. Mahler, *Quantum Thermodynamics* (Springer-Verlag Berlin Heidelberg, 2009), Vol. 784.
- [54] M. Horodecki and J. Oppenheim, Fundamental limitations for quantum and nanoscale thermodynamics, *Nature Commun.* **4**, 2159 (2013).
- [55] Z. Wang, L. Wang, J. Chen, C. Wang and J. Rie, Geometric heat pump: Controlling thermal transport with time-dependent modulations, *Frontier, Phys.* **17**, 13201 (2022).
- [56] K. Brandner and K. Saito, Thermodynamic Geometry of Microscopic Heat Engines Kay Brandner and Keiji Saito, *Phys. Rev. Lett.* **124**, 040602 (2020).
- [57] S. K. Giri and H. P. Goswami, Geometric phaselike effects in a quantum heat engine, *Phys. Rev. E* **96**, 052129 (2017), *ibid* **99**, 022104 (2019).
- [58] Y. Hino and H. Hayakawa, Geometric formulation of adiabatic pumping as a heat engine, *Phys. Rev. Research* **3**, 013187 (2021).
- [59] B. Bhandari, P. T. Alonso, F. Taddei, F. von Oppen, R. Fazio and L. Arrachea, Geometric properties of adiabatic quantum thermal machines, *Phys. Rev. B* **102**, 155407 (2020),
- [60] P. Abiuso, H. J. D. Miller, M. Perarnau-Llobet, and M. Scandi, Geometric optimisation of quantum thermodynamic processes, *Entropy* **22**, 1076 (2020).
- [61] P. T. Alonso, P. Abiuso, M. Perarnau-Llobet, and L. Arrachea, Geometric Optimization of Nonequilibrium Adiabatic Thermal Machines and Implementation in a Qubit System, *PRX Quantum* **3**, 010326 (2022) .
- [62] J. Eglinton and K. Brandner, Geometric bounds on the power of adiabatic thermal machines, *Phys. Rev. E* **105**, L052102 (2022) .
- [63] Z. Wang and J. Rie, Thermodynamic Geometry of Nonequilibrium Fluctuations in Cyclically Driven Transport *Phys. Rev. Lett.* **132**, 207101 (2024).
- [64] R. Yoshii and H. Hayakawa, Daemon driven by geometric phase, *Phys. Rev. Research*, **5**, 033014 (2023).
- [65] R. Yoshii and H. Hayakawa, Analytical expression of geometric pumping for a quantum dot based on quantum master equation, arXiv:1312.3772
- [66] S. Kullback, and R. A. Leibler, On information and sufficiency, *Annal. Math. Stat.*, **22**, 79 (1951).
- [67] T. Sagawa, Entropy, Divergence, and Majorization in Classical and Quantum Thermodynamics, (Springer-Brief in Mathematical Physics, Springer, Singapore, 2022). See also arXiv:2007.09974.
- [68] G. Lindblad, On the generators of quantum dynamic semigroups, *Commun. Math. Phys.* **119**, 48 (1976).
- [69] D. Manzano, A short introduction to the Lindblad Master Equation, *AIP Advances* **10**, 025106 (2020).
- [70] K. Mizuta, K. Takasan and N. Kawakami, Breakdown of Markovianity by interactions in stroboscopic Floquet-Lindblad dynamics under high-frequency drive *Phys. Rev. A* **103**, L020202 (2021).
- [71] H.-P. Breuer, E.-M. Laine, J. Piilo, and B. Vacchini, Non-Markovian dynamics in open quantum systems, *Rev. Mod. Phys.* **88**, 021002 (2016).
- [72] K Takahashi, K Fujii, Y Hino, and H Hayakawa, Nonadiabatic Control of Geometric Pumping, *Phys. Rev. Lett.* **124**, 150602 (2020).
- [73] K. Funo, N. Lambert, F. Nori, and C. Flindt, Shortcuts to Adiabatic Pumping in Classical Stochastic Systems *Phys. Rev. Lett.* **124**, 150603 (2020).
- [74] P. Strasberg, *Quantum Stochastic Thermodynamics: Foundations and Selected Applications* (Oxford Univ. Press, Oxford, 2022).
- [75] G. Benenti, G. Casati, K. Saito, and R. S. Whitney, *Phys. Rep.* **694**, 1 (2017).
- [76] G. Kurizki and A. G. Kofman, *Thermodynamics and Control of Open Quantum Systems* (Cambridge Univ. Press, Cambridge, 2022).
- [77] R. Baruah, P. Portugal, J. Wabnig, and C. Flindt, Fast, accurate, and local temperature control using qubits *Phys. Rev.*

- B, **111**, 125406 (2025).
- [78] P. Abiuso, H. J. D. Miller, M. Perarnau-Llobet, and M. Scandi, Geometric Optimisation of Quantum Thermodynamic Processes Entropy **22**, 1076 (2020)
- [79] A. A. Svidzinsky, K. E. Dorfman, M. O. Scully, Enhancing photocell power by noise-induced coherence, Coherent Opt. Phenomena, **1**, 7 (2012).
- [80] H. Tajima, and K. Funo, Superconducting-like Heat Current: Effective Cancellation of Current-Dissipation Trade-Off by Quantum Coherence, Phys. Rev. Lett. **127**, 190604 (2021).
- [81] K. Viebahn, A.-S. Walter, E. Bertok, Z. Zhu, M. Gächter, A. A. Aligia, F. Heidrich-Meisner, and T. Esslinger, Interactions Enable Thouless Pumping in a Non-sliding Lattice. Phys. Rev. X **14**, 021049 (2024).
- [82] Walter, A.S., Zhu, Z., Gächter, M. *et al.*, Quantization and its breakdown in a Hubbard–Thouless pump. Nat. Phys. **19**, 1471 (2023).
- [83] Y. Liu, Y.R. Zhang, Y.H. Shi, *et al.*, Interplay between disorder and topology in Thouless pumping on a superconducting quantum processor. Nat. Commun. **16**, 108 (2025).
- [84] S. Nakajima, M. Taguchi, T. Kubo and Y. Tokura, Interaction effect on adiabatic pump of charge and spin in quantum dot Phys. Rev. B **92**, 195420 (2015).
- [85] M. Leijnse and M. R. Wegewijs, Kinetic equations for transport through single-molecule transistors, Phys. Rev. B **78**, 235424 (2008).